

Conserving mass, momentum, and energy for the Benjamin-Bona-Mahony, Korteweg-de Vries, and nonlinear Schrödinger equations

Hendrik Ranocha^{*1} and David I. Ketcheson⁺²

¹Institute of Mathematics, Johannes Gutenberg University Mainz, Staudingerweg 9, 55128 Mainz, Germany

²King Abdullah University of Science and Technology (KAUST), Computer Electrical and Mathematical Science and Engineering Division (CEMSE), Thuwal, 23955-6900, Saudi Arabia

December 19, 2025

We propose and study a class of arbitrarily high order numerical discretizations that preserve multiple invariants and are essentially explicit (they do not require the solution of any large systems of algebraic equations). In space, we use Fourier Galerkin methods, while in time we use a combination of orthogonal projection and relaxation. We prove and numerically demonstrate the conservation properties of the method by applying it to the Benjamin-Bona-Mahoney, Korteweg-de Vries, and nonlinear Schrödinger (NLS) PDEs as well as a hyperbolic approximation of NLS. For each of these equations, the proposed schemes conserve mass, momentum, and energy up to numerical precision. We show that this conservation leads to reduced growth of numerical errors for long-term simulations.

Key words. Fourier Galerkin methods, additive Runge-Kutta methods, structure-preserving methods, Benjamin-Bona-Mahony equation, Korteweg-de Vries equation, nonlinear Schrödinger equation

AMS subject classification. 65M60, 65M70, 65M12, 65M20

1 Introduction

Many important partial differential equations (PDEs) possess conserved quantities (such as mass, momentum, or energy) that are fundamental properties of the corresponding physical system. Preserving these invariants by numerical methods is essential not only in obtaining accurate solutions but also to ensure that the solutions are physically meaningful at all. Therefore, great effort has gone into the development of *structure-preserving* numerical methods. Most often, such methods are designed to preserve one, or in some cases, two such invariants. However, many models possess more than two invariants; indeed, fully integrable systems (such as the Korteweg-de Vries or nonlinear Schrödinger equations) possess infinitely many.

^{*}ORCID: 0000-0002-3456-2277

[†]ORCID: 0000-0002-1212-126X

In this work we present a class of full (space and time) discretizations that conserve three invariants (mass, momentum, and energy) for three of the most important nonlinear dispersive wave models: the Benjamin-Bona-Mahony (BBM), Korteweg-de Vries (KdV), and nonlinear Schrödinger (NLS) equations. For periodic boundary conditions, each of these equations conserves the total mass \mathcal{M} , momentum \mathcal{P} , and energy \mathcal{E} given as follows.

The Benjamin-Bona-Mahony equation¹ [13]

$$u_t + uu_x - u_{txx} = 0 \quad (1.1)$$

has the three invariants [70]

$$\mathcal{M} = \int u \, dx, \quad \mathcal{P} = \int \left(\frac{1}{2}u^2 + \frac{1}{2}(u_x)^2 \right) dx, \quad \mathcal{E} = \int \frac{1}{6}u^3 \, dx. \quad (1.2)$$

The Korteweg-de Vries equation [57]

$$u_t + uu_x + u_{xxx} = 0 \quad (1.3)$$

has a countably infinite number of invariants [67]; the first three of them are

$$\mathcal{M} = \int u \, dx, \quad \mathcal{P} = \int \frac{1}{2}u^2 \, dx, \quad \mathcal{E} = \int \left(\frac{1}{2}(u_x)^2 - \frac{1}{6}u^3 \right) dx. \quad (1.4)$$

The nonlinear Schrödinger equation [89, 95]

$$iu_t + u_{xx} + \beta|u|^2u = 0 \quad (1.5)$$

also has infinitely many invariants. The first three of them are

$$\mathcal{M} = \int |u|^2 \, dx, \quad \mathcal{P} = \int \text{Im}(\bar{u}u_x) \, dx, \quad \mathcal{E} = \int \left(|u_x|^2 - \frac{\beta}{2}|u|^4 \right) dx. \quad (1.6)$$

Our approach employs the widely-used method of lines, in which PDEs are discretized in space and the resulting ordinary differential equation (ODE) system is then integrated. In order to preserve an invariant at the fully-discrete level within this framework, both the spatial and the temporal discretization must be conservative. Due to the spatial discretization, the quantity conserved by the numerical method is some discrete approximation of the original invariant.

1.1 Spatial discretizations

Since conservation of invariants can be proven using integration by parts, many conservative spatial discretizations are created by mimicking this procedure at the discrete level, either using a Galerkin approach (assuming exact integration of all nonlinear terms) or by using summation-by-parts (SBP) operators [36, 90]. While SBP-based methods can be constructed to conserve two invariants for the equations of interest [63, 77, 78, 81], they do not appear to be able to conserve three or more invariants. The underlying reason for this is that SBP discretizations conserving the total mass are based on split forms of the nonlinear terms, which are related to entropy-conserving methods for conservation laws in the classical setting of Tadmor [91, 92]. The nonlinear term of the BBM/KdV equation is the same as in Burgers' equation $u_t + (u^2/2)_x = 0$. Using Tadmor's theory, we can construct numerical fluxes that can either conserve the quadratic invariant $\int u^2/2$ or the cubic invariant $\int u^3/6$, but not both at the same time (since entropy-conservative fluxes are determined uniquely for scalar conservation laws).

¹This equation is often written with an additional linear term $+u_x$, which can be removed by the transformation $u \mapsto u - 1$ to obtain the normalization also used in [21, 41].

One alternative approach to construct spatial discretizations conserving multiple invariants is to use a reasonable baseline discretization and add correction terms enforcing the desired conservation properties [1, 3]. In this vein, Chen et al. [25] introduced local discontinuous Galerkin (LDG) methods for KdV with additional unknown stabilization parameters to enforce conservation of the first three invariants. However, initial numerical experiments in which we have extended this approach to fully-discrete conservation suggest that this approach is less robust in practice, at least when combined with the temporal discretizations described below.

The Ablowitz-Ladik lattice [4, Ch. 3] can also be viewed as a spatial discretization of NLS that possesses an infinite set of conserved quantities related to those of NLS.

Here we turn instead to Galerkin methods. Many classical finite element schemes use piecewise polynomials with a prescribed degree of regularity at cell boundaries; since the derivative of such a polynomial does not lie in the same space (it has lower regularity), such methods cannot be used to conserve invariants involving derivatives. However, Fourier Galerkin methods are promising since the derivative is an endomorphism on the space of trigonometric polynomials. Indeed, Maday and Quarteroni [64, Lemma II.1] showed that the Fourier Galerkin method conserves the first three KdV invariants. Here we extend this result to the NLS and BBM equations, and provide efficient time discretizations that lead to a fully-discrete conservative scheme.

1.2 Temporal discretizations

For temporal conservation of invariants, the literature on structure-preserving ODE integrators is extensive; for an overview we refer the reader to the monograph [45]. We will highlight some of the most relevant approaches. Linear or affine invariants are automatically preserved by the most common types of discretizations, e.g., general linear methods such as Runge-Kutta methods and linear multistep methods. Special implicit methods can be designed to conserve quadratic invariants (symplectic methods [45, Sections IV.2 and VI.7]) or to preserve the Hamiltonian in the case of Hamiltonian systems (e.g., discrete gradient methods or the average vector field method [24, 44, 65, 73]). We mention here also the scalar auxiliary variable (SAV) method (e.g., [62]) in which the equations to be solved are augmented by one or more additional equations related to the conserved quantity or quantities. For more general invariants, one can simply project the solution back onto the conservative manifold after each step. This can be done using orthogonal projection [45, Section IV.4] or by projecting along a line determined by the numerical ODE solver; the latter approach is known as relaxation [53, 80, 83].

The basic idea of relaxation methods dates back to [86] and [29, pp. 265–266], and has recently been developed in a general setting in [53, 80, 83]. It has been combined with Runge-Kutta methods [83], linear multistep methods [80], residual distribution schemes [2], IMEX methods [51, 60], and multi-derivative methods [84, 85]. Some applications include Hamiltonian problems [59, 78, 97], compressible flows [33, 75, 94], dispersive wave equations [58, 61, 66, 82], and asymptotic-preserving methods for hyperbolizations [20, 21, 42]. The advantage of such methods is that they can be essentially explicit, requiring only the solution of a scalar nonlinear equation at each step. The relaxation approach has been extended in order to conserve multiple invariants [18, 19], although the resulting method is more costly and less robust, occasionally requiring the use of small timesteps.

The time discretization we use in the present work is an extension of our previous work [77], in which we combine orthogonal projection with relaxation to conserve mass, momentum, and energy for the BBM, KdV, and NLS equations.

1.3 Full discretizations

From the large body of literature on structure-preserving methods for the BBM, KdV, and NLS equations, we are only aware of two (rather recent) papers developing fully-discrete methods conserving mass, momentum, and energy for one of these equations: Zheng and Xu [98] use a

fully implicit LDG method with Lagrange multipliers and a spectral deferred correction approach for the KdV equation, and Akrivis et al. [6] use a fully-implicit space-time finite element method with Lagrange multipliers for the NLS equation. In contrast to these methods, our schemes are less implicit and more flexible in terms of the choice of the temporal discretization. Instead of designing a conservative spatial scheme, for one-dimensional problems with smooth enough solutions one can simply use a highly resolved Fourier collocation method that is essentially exact (up to machine precision). Alvarez et al. [8] combined this with projection methods in time applied to an SDIRK method to conserve mass, momentum, and energy for the KdV equation.

We cannot provide a complete overview of all papers on structure-preserving methods for the BBM, KdV, and NLS equations here. However, we will briefly summarize some related literature and apologize for any omissions.

There are some general methodological developments that have been applied to several equations. Discrete variational derivative methods can be used to conserve two invariants of BBM, KdV, and NLS [40, 55]. Frasca-Caccia and Hydon have designed bespoke finite difference methods conserving local forms of the conservation laws for two invariants for BBM, KdV, and NLS [37, 38].

There are many methods conserving two invariants at the fully discrete level. For the NLS equation, some mass- and energy-conserving methods are studied in [7, 12, 14, 15, 18, 26, 30, 46, 77, 87]; methods conserving the mass and the Hamiltonian structure are analyzed in [23]. SBP operators can be combined with relaxation to conserve mass and either momentum or energy for the BBM and KdV equations [63, 78, 81] and their hyperbolic approximations [20, 21]. The SAV method can be used to conserve mass, momentum, and a modified energy for generalized KdV equations [96].

Fourier Galerkin space discretization has recently been combined with a symplectic RK time discretization to achieve fully-discrete conservation of the linear and quadratic invariants [34]. Andrews and Farrel [9] have developed fully implicit time integration methods able to conserve multiple invariants (up to quadrature and solver tolerances), and applied the procedure to conserve the energy of the BBM equation.

There are also techniques that directly develop a conservative space-time discretization; these include Grant's method [37, 43], the discrete variational derivative method [40], and the discrete multiplier method [88, 93]. In principle these approaches could be applied to conserve an arbitrary number of invariants, but in practice conserving more than two leads to major difficulties, and has not been demonstrated.

1.4 Contributions and outline

As we can see from the foregoing, most structure-preserving methods have one or more of the following drawbacks: they conserve only one or two invariants, they are limited to second order, and they require the solution of large systems of algebraic equations. Here we provide methods that combine the following advantages:

- conservation of mass, momentum, and energy;
- arbitrary order in space and time;
- only a scalar equation must be solved at each step.

An additional advantage of the present approach is that we can use any baseline method, e.g., an IMEX method for the KdV and NLS equations to handle the stiff linear terms efficiently, and an explicit method for the non-stiff BBM equation.

The most important restrictions of these new methods are that they require periodic boundary conditions and they provide only global (not local) conservation.

In Section 2 we focus on spatial discretization, showing that Fourier Galerkin methods provide the desired conservation properties. We also point out some crucial subtleties to obtain the desired results in (acceptably efficient) implementations, and demonstrate the semidiscrete conservation

numerically. In Section 3 we introduce our conservative time discretization method, which combines orthogonal projection with relaxation and is an extension of that proposed in our recent work [77]. Fully-discrete conservation is demonstrated through numerical experiments. In Section 4 we study the long-term error behavior of our conservative methods compared with methods that conserve fewer invariants. In Section 5 we perform a practical comparison of computational efficiency between our proposed methods and some recent methods from the literature. In Section 6 we apply the same ideas to a first-order hyperbolic approximation of NLS. Some conclusions and future directions are discussed in Section 7.

2 Spatial semidiscretizations

We use Fourier Galerkin methods to discretize the PDEs in space. Let T_k be the space of real-valued trigonometric polynomials of degree at most k and let P be the L^2 projection² onto T_k . We denote the L^2 inner product on the spatial domain by $\langle \cdot, \cdot \rangle$. Next, we will introduce the resulting semidiscretizations and prove that they conserve the mass, momentum, and energy for each equation.

2.1 Benjamin-Bona-Mahony equation

The Fourier Galerkin semidiscretization of the BBM equation (1.1) is given by

$$\partial_t u = -(I - \partial_x^2)^{-1} \partial_x P \frac{u^2}{2}. \quad (2.1)$$

Theorem 2.1. *The semidiscretization (2.1) of the BBM equation (1.1) conserves the mass, momentum, and energy (1.2).*

Proof. The semidiscretization (2.1) conserves the total mass $\mathcal{M} = \int u \, dx$, since

$$\partial_t \mathcal{M} = \langle 1, \partial_t u \rangle = - \left\langle 1, (I - \partial_x^2)^{-1} \partial_x P \frac{u^2}{2} \right\rangle = \left\langle (I - \partial_x^2)^{-1} \partial_x 1, P \frac{u^2}{2} \right\rangle = 0, \quad (2.2)$$

where we used the skew-symmetry of $(I - \partial_x^2)^{-1} \partial_x$ in the second-to-last step and $\partial_x 1 = 0$ in the last step. Similarly, it conserves the momentum $\mathcal{P} = \int (u^2 + u_x^2)/2 \, dx = \int u(I - \partial_x^2)u/2 \, dx$, since

$$\begin{aligned} 2\partial_t \mathcal{P} &= 2 \left\langle (I - \partial_x^2)u, \partial_t u \right\rangle = - \left\langle (I - \partial_x^2)u, (I - \partial_x^2)^{-1} \partial_x P u^2 \right\rangle \\ &= \left\langle \partial_x u, P u^2 \right\rangle = \left\langle \partial_x u, u^2 \right\rangle = 0, \end{aligned} \quad (2.3)$$

where we used that $\partial_x u \in T_k$ in the second-to-last step so that we can use the chain rule in the last step. Moreover, the total energy $\mathcal{E} = \int u^3/6 \, dx$ is also conserved, since

$$4\partial_t \mathcal{E} = 2 \left\langle u^2, \partial_t u \right\rangle = - \left\langle u^2, (I - \partial_x^2)^{-1} \partial_x P u^2 \right\rangle = - \left\langle P u^2, (I - \partial_x^2)^{-1} \partial_x P u^2 \right\rangle = 0, \quad (2.4)$$

where we used that the semidiscrete rate of change $\partial_t u \in T_k$ in the second-to-last step and the skew-symmetry of $(I - \partial_x^2)^{-1} \partial_x$ in the last step. \square

²We omit the index k from P since we will only use a fixed k in each equation, not multiple spaces.

2.2 Korteweg-de Vries equation

The Fourier Galerkin semidiscretization of the KdV equation (1.3) is given by

$$\partial_t u = -\partial_x P \frac{u^2}{2} - \partial_x^3 u. \quad (2.5)$$

Theorem 2.2 (Maday and Quarteroni [64]). *The semidiscretization (2.5) of the KdV equation (1.3) conserves the mass, momentum, and energy (1.4).*

Proof. The semidiscretization (2.5) conserves the total mass $\mathcal{M} = \int u \, dx$, since

$$\partial_t \mathcal{M} = \langle 1, \partial_t u \rangle = - \left\langle 1, \partial_x P \frac{u^2}{2} \right\rangle - \left\langle 1, \partial_x^3 u \right\rangle = \left\langle \partial_x 1, P \frac{u^2}{2} \right\rangle + \left\langle \partial_x^3 1, u \right\rangle = 0. \quad (2.6)$$

Similarly, it conserves the momentum $\mathcal{P} = \int u^2/2 \, dx$, since

$$\partial_t \mathcal{P} = \langle u, \partial_t u \rangle = - \left\langle u, \partial_x P \frac{u^2}{2} \right\rangle - \left\langle u, \partial_x^3 u \right\rangle = \left\langle \partial_x u, \frac{u^2}{2} \right\rangle + \left\langle \partial_x^3 u, u \right\rangle = 0, \quad (2.7)$$

where we used that $\partial_x u \in T_k$ in the second-to-last step so that we can use the chain rule in the last step. Moreover, the total energy $\mathcal{E} = \int (u_x^2/2 - u^3/6) \, dx = - \int (u \partial_x^2 u/2 + u^3/6) \, dx$ is also conserved, since

$$\begin{aligned} \partial_t \mathcal{E} &= - \left\langle \partial_x^2 u + \frac{u^2}{2}, \partial_t u \right\rangle \\ &= \left\langle \partial_x^2 u, \partial_x P \frac{u^2}{2} \right\rangle + \left\langle \frac{u^2}{2}, \partial_x P \frac{u^2}{2} \right\rangle + \left\langle \partial_x^2 u, \partial_x^3 u \right\rangle + \left\langle \frac{u^2}{2}, \partial_x^3 u \right\rangle \\ &= - \left\langle \partial_x^3 u, P \frac{u^2}{2} \right\rangle + \left\langle P \frac{u^2}{2}, \partial_x P \frac{u^2}{2} \right\rangle + 0 + \left\langle P \frac{u^2}{2}, \partial_x^3 u \right\rangle = 0, \end{aligned} \quad (2.8)$$

where we used the skew-symmetry of ∂_x . \square

Remark 2.3. The Fourier Galerkin semidiscretization (2.5) of the KdV equation (1.3) does not conserve the fourth invariant given by

$$\begin{aligned} \partial_t \left(\frac{1}{24} u^4 - \frac{1}{2} u u_x^2 + \frac{3}{10} u_{xx}^2 \right) + \partial_x \left(\frac{1}{30} u^5 + \frac{1}{6} u^3 u_{xx} - \frac{3}{4} u^2 u_x^2 - u u_x u_{xxx} \right. \\ \left. + \frac{4}{5} u u_{xx}^2 + \frac{1}{2} u_x^2 u_{xx} + \frac{3}{5} u_{xx} u_{xxxx} - \frac{3}{10} u_{xxx}^2 \right) = 0. \end{aligned} \quad (2.9)$$

We did not check whether other higher-order invariants are conserved. \triangleleft

2.3 Nonlinear Schrödinger equation

To formulate the semidiscretization of the NLS equation (1.5), we rewrite it as a system for the real and imaginary parts $u = v + iw$:

$$\begin{aligned} v_t + w_{xx} + \beta(v^2 + w^2)w &= 0, \\ w_t - v_{xx} - \beta(v^2 + w^2)v &= 0. \end{aligned} \quad (2.10)$$

The invariants (1.6) can be rewritten as

$$\begin{aligned}\mathcal{M} &= \int (v^2 + w^2) dx, & \mathcal{P} &= \int (vw_x - wv_x) dx = 2 \int vw_x dx, \\ \mathcal{E} &= \int \left(v_x^2 + w_x^2 - \frac{\beta}{2} (v^2 + w^2)^2 \right) dx.\end{aligned}\tag{2.11}$$

The Fourier Galerkin semidiscretization of (2.10) is given by

$$\begin{aligned}\partial_t v &= -w_{xx} - \beta P(v^2 + w^2)w, \\ \partial_t w &= v_{xx} + \beta P(v^2 + w^2)v.\end{aligned}\tag{2.12}$$

Theorem 2.4. *The semidiscretization (2.12) of the NLS equation (2.10) conserves the mass, momentum, and energy (2.11).*

Proof. The semidiscretization (2.12) conserves the total mass $\mathcal{M} = \int (v^2 + w^2) dx$, since

$$\begin{aligned}\partial_t \mathcal{M} &= 2 \langle v, \partial_t v \rangle + 2 \langle w, \partial_t w \rangle \\ &= -2 \langle v, w_{xx} + \beta P(v^2 + w^2)w \rangle + 2 \langle w, v_{xx} + \beta P(v^2 + w^2)v \rangle = 0,\end{aligned}\tag{2.13}$$

where we used the symmetry of ∂_x^2 and exactness of the L^2 projection P in the last step. Similarly, the semidiscretization conserves the momentum $\mathcal{P} = 2 \int vw_x dx$, since

$$\begin{aligned}\partial_t \mathcal{P} &= 2 \langle w_x, \partial_t v \rangle - 2 \langle v_x, \partial_t w \rangle \\ &= -2 \langle w_x, w_{xx} + \beta P(v^2 + w^2)w \rangle - 2 \langle v_x, v_{xx} + \beta P(v^2 + w^2)v \rangle \\ &= -2\beta \int (v^2 + w^2)(ww_x + vv_x) dx = -\frac{1}{2}\beta \int \partial_x(v^2 + w^2)^2 dx = 0,\end{aligned}\tag{2.14}$$

where we used the anti-symmetry of ∂_x and exactness of the L^2 projection P . Finally, the total energy $\mathcal{E} = \int (v_x^2 + w_x^2 - \beta(v^2 + w^2)^2/2) dx = - \int (v\partial_x^2 v + w\partial_x^2 w + \beta(v^2 + w^2)^2/2) dx$ is also conserved, since

$$\begin{aligned}\partial_t \mathcal{E} &= -2 \langle v_{xx} + \beta(v^2 + w^2)v, \partial_t v \rangle - 2 \langle w_{xx} + \beta(v^2 + w^2)w, \partial_t w \rangle \\ &= 2 \langle v_{xx} + \beta P(v^2 + w^2)v, w_{xx} + \beta P(v^2 + w^2)w \rangle \\ &\quad - 2 \langle w_{xx} + \beta P(v^2 + w^2)w, v_{xx} + \beta P(v^2 + w^2)v \rangle = 0,\end{aligned}\tag{2.15}$$

where we used again $\partial_t v, \partial_t w \in T_k$ and the exactness of the L^2 projection P . \square

2.4 Implementation notes

Since we work with real-valued functions, we use the forward/backward real FFT (in FFTW [39]) to map between spatial values and modal coefficients. While it is often convenient to use the spatial coordinates as the primary representation (which can be visualized directly), we cannot do so if an even number of nodes is used; in this case, the backward real FFT drops the imaginary part of the highest mode (Nyquist frequency) to ensure that the output is real-valued. This loss of information cannot be recovered later and destroys the structures we used to prove conservation. Thus, we use the modal coefficients as primary variables and compute the spatial derivatives by multiplying all modes by the appropriate (powers of the) imaginary unit and wave number. Please note that this differs from the common practice to set the Nyquist frequency of odd-derivative operators to zero for an even number of nodes [49]. However, it is required to obtain the desired conservation of the mass, momentum, and energy for an even number of nodes.

To compute the exact L^2 projection P , we use a classical de-aliasing strategy. Assume we have a polynomial nonlinearity of degree p and N spatial nodes to represent u . First, we use the modal coefficients of u and extend them by zero to obtain the modal coefficients of the representation of u with M nodes. Then, we compute the nodal values on these M nodes, compute the nonlinearity in physical space, compute the modal coefficients of the result on M nodes, and truncate them back to the modal coefficients corresponding to N nodes. This ensures that we obtain the exact L^2 projection of the degree p nonlinearity if $M > (p+1)N/2$, see, e.g., [56, Section 4.3.2] for a detailed description of the case $p = 2$ and [31, 50] for general p . For quadratic nonlinearities with $p = 2$, this is the well-known 3/2-rule [71].

To improve the efficiency, we compute a minimal number M_{\min} of nodes to achieve de-aliasing based on the rules above. Then, we choose $M \geq M_{\min}$ as the smallest integer with prime factors in $\{2, 3, 5, 7\}$. To further improve the performance of the implementations, we use several larger grids (with $M > N$ nodes) to compute the nonlinearities in physical space, e.g., based on a factor 3/2 for the quadratic nonlinearities uu_x in the BBM and KdV equations and a factor 2 for the cubic nonlinearities in the energies of these equations. We initialize the numerical solution by sampling the initial condition at N nodes and computing the corresponding modal coefficients.

We implemented all methods in Julia [16]. We use FFTW.jl [39] wrapped in SummationByPartsOperators.jl [74] for the Fourier Galerkin methods. The visualizations are created using Makie.jl [27]. All code and data required to reproduce the numerical results are available online in our reproducibility repository [79].

2.5 Numerical verification of the semidiscrete invariant conservation

Next, we verify the conservation of the mass, momentum, and energy for the semidiscretizations of the BBM, KdV, and NLS equations numerically. While explicit solitary wave (soliton) solutions are available for all three equations, a single solitary wave is often not challenging enough to demonstrate conservation of multiple invariants. Thus, we use setups with two interacting waves for each equation.

The BBM equation (1.1) has solitary wave solutions

$$u_{x_0,c}(t, x) = 1 + A \cosh(k(x - x_0 - ct))^{-2}, \quad A = 3(c - 1), \quad k = \frac{1}{2}\sqrt{1 - 1/c}. \quad (2.16)$$

We initialize the numerical solution as

$$u(0, x) = u_{-20,1.3}(0, x) + u_{20,1.2}(0, x) - 1 \quad (2.17)$$

in the domain $[-100, 100]$ with periodic boundary conditions and choose a time span of $[0, 400]$ to ensure that the two waves interact with each other.

The KdV equation (1.3) has the two-soliton solution [47, 48]

$$u(t, x) = 12\partial_x^2 \log F, \quad F = 1 + e^{\eta_1} + e^{\eta_2} + a_{12}e^{\eta_1 + \eta_2}, \quad \eta_i = k_i(x - x_{i,0}) - k_i^3 t. \quad (2.18)$$

We choose the parameters

$$k_1 = 0.75, \quad k_2 = 0.5, \quad x_{1,0} = -50, \quad x_{2,0} = 50, \quad (2.19)$$

and the spatial domain $[-200, 200]$ with periodic boundary conditions. The time span $[0, 350]$ ensures that the two waves interact. We use Enzyme.jl [68, 69] to compute the second-derivative via automatic/algorithmic differentiation (AD).

For the NLS equation (1.5), we use the same two-soliton solution as in [18, 77]; we choose the spatial domain $[-35, 35]$ with periodic boundary conditions and the time span $[0, 10]$.

For all three equations, we use coarse meshes with $N \in \{31, 32\}$ nodes and sufficiently small time step sizes to ensure that the errors in time are negligible. The results are shown in Figure 1. As expected, the Fourier Galerkin semidiscretizations conserve all three invariants up to the precision of the time integration method (which is close to machine accuracy due to the choice of sufficiently small time step sizes Δt).

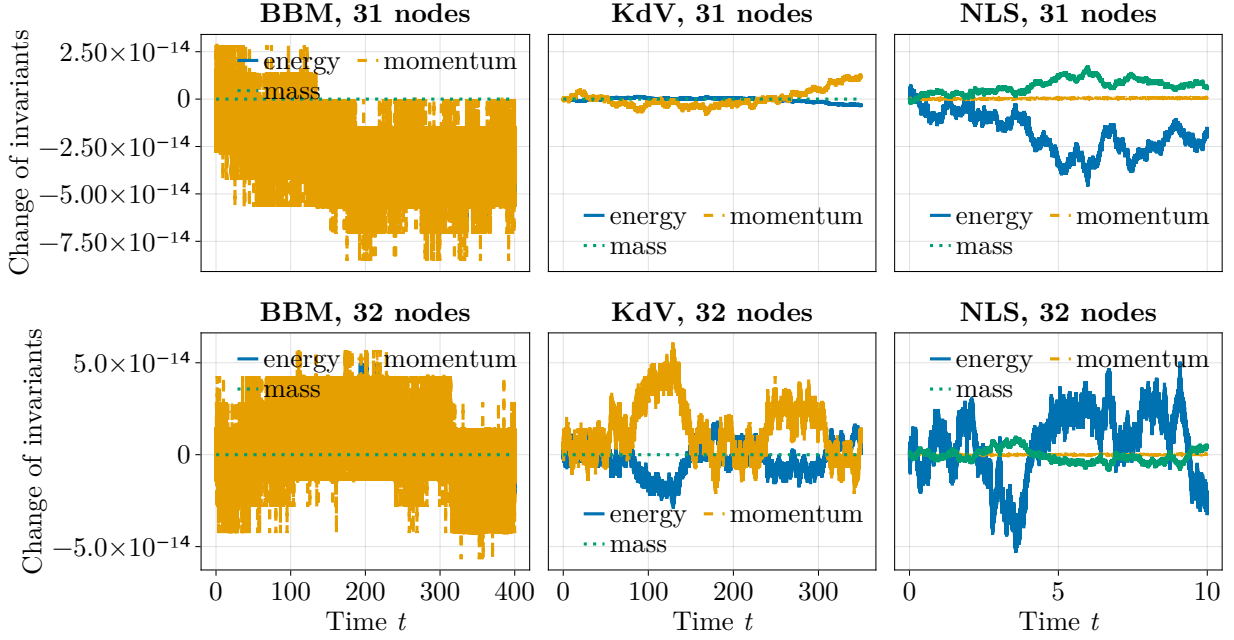


Figure 1: Change of invariants over time for the Fourier Galerkin semidiscretizations of the BBM, KdV, and NLS equations with two interacting solitary waves. The time integration is performed with the fifth-order method of [52] with $\Delta t = 5 \times 10^{-3}$ for the BBM, $\Delta t = 1 \times 10^{-2}$ for the KdV, and $\Delta t = 1 \times 10^{-4}$ for the NLS equation.

3 Time discretizations

General linear methods like Runge-Kutta (RK) methods and linear multistep methods typically conserve only the linear invariants, e.g., the total mass \mathcal{M} of the BBM and KdV equations. While there are some special combinations of methods and problems where simple explicit schemes conserve a nonlinear invariant [76, Section 5], this cannot be expected in general. Quadratic invariants like the momentum \mathcal{P} for the BBM, KdV, and NLS equations are conserved by symplectic Runge-Kutta methods, which are necessarily fully implicit [45].

We want to avoid fully implicit methods due to the high computational costs of solving large nonlinear systems. Thus, we use implicit-explicit (IMEX) additive Runge-Kutta (ARK) methods [11, 52], which treat the linear stiff terms of the KdV and NLS equations implicitly and all nonlinear terms explicitly (for the BBM equation, we only use the explicit parts of the ARK methods). Since we use Fourier methods in space, the resulting linear systems can be solved efficiently in modal space.

To enforce conservation of all invariants, we use the quadratic-preserving relaxation method from [77]. It combines an orthogonal projection (see, e.g., [22] or [45, Section IV.4]) with relaxation (see, e.g., [80, 83]). For an ODE

$$u'(t) = f(u(t)) \quad (3.1)$$

with invariant (first integral) η satisfying $\forall u: \eta'(u)f(u) = 0$, the quadratic-preserving relaxation method [77] performs the following steps:

- Given $u^n \approx u(t^n)$, compute a provisional value $\tilde{u}^{n+1} \approx u(\tilde{t}^{n+1})$ using a baseline time integration method, e.g., an ARK method.
- Project the baseline result onto the manifold defined by a quadratic invariant using the projection operator π , i.e., compute $\hat{u}^{n+1} = \pi(\tilde{u}^{n+1})$.
- Search for a solution conserving the additional invariant η along the (approximate) geodesic

line connecting u^n and \hat{u}^{n+1} , i.e., solve the scalar equation

$$\eta\left(\pi(u^n + \gamma(\hat{u}^{n+1} - u^n))\right) = \eta(u^n) \quad (3.2a)$$

for the scalar relaxation parameter γ .

- Continue the numerical time integration with

$$u^{n+1} = \pi(u^n + \gamma(\hat{u}^{n+1} - u^n)) \approx u(t^{n+1}), \quad t^{n+1} = t^n + \gamma\Delta t, \quad (3.2b)$$

instead of \hat{u}^{n+1} and \tilde{t}^{n+1} .

For the nonlinear Schrödinger equation considered in [77], the projection operator conserving the mass from one step to the next is given by

$$\pi(\tilde{u}^{n+1}) = \sqrt{\frac{\mathcal{M}(u^n)}{\mathcal{M}(\tilde{u}^{n+1})}}\tilde{u}^{n+1}. \quad (3.3)$$

By construction, the invariant enforced by π and the invariant η are conserved. In [77], η is chosen as the energy \mathcal{E} of the NLS equation.

We generalize this approach by choosing the projection operator π to conserve both the mass \mathcal{M} and the momentum \mathcal{P} . This allows us to construct relaxation methods conserving all three invariants of the BBM, KdV, and NLS equations by choosing η as the energy \mathcal{E} . From [77], we have

Theorem 3.1. *Assume that the ODE (3.1) has the invariants $(\mathcal{M}, \mathcal{P}, \mathcal{E})$ and that π is a projection operator onto the manifold defined by the two constraints $\mathcal{M}(u) = \mathcal{M}(u^n)$ and $\mathcal{P} = \mathcal{P}(u^n)$. Let $\eta = \mathcal{E}$ and assume that the baseline one-step method is of order $p \geq 2$ and that*

$$\eta'(u^n)\pi'(u^n)f'(u^n)f(u^n) \neq 0. \quad (3.4)$$

Then, the generalized quadratic-preserving relaxation method (3.2) is well-defined for sufficiently small time step sizes Δt ; there is a unique solution of (3.2a) with $\gamma = 1 + O(\Delta t^{p-1})$ and the resulting order of accuracy is at least p (when measuring the error at the relaxed time $t^{n+1} = t^n + \gamma\Delta t$). Moreover, all three invariants are conserved.

The non-degeneracy condition (3.4) is a generalization of similar conditions for standard relaxation methods and is discussed further in [77]. For example, it ensures that u^n is not a steady state of the ODE.

In practice, we solve the scalar nonlinear equation for γ using the method of [54] implemented in SimpleNonlinearSolve.jl [72].

3.1 Implementation of the projection operators

For the BBM and KdV equations, the mass \mathcal{M} is a linear invariant, while the momentum \mathcal{P} is a quadratic invariant and induces a norm. Using this norm to measure distances, the orthogonal projection onto the manifold defined by constant mass and momentum is given by

$$\pi(u^{n+1}) = \bar{u} + \sqrt{\frac{\mathcal{P}(u^n) - \mathcal{P}(\bar{u})}{\mathcal{P}(u^{n+1}) - \mathcal{P}(\bar{u})}}(u^{n+1} - \bar{u}), \quad (3.5)$$

where

$$\bar{u} = \frac{\mathcal{M}(u^n)}{\mathcal{M}(1)} = \frac{\mathcal{M}(u^{n+1})}{\mathcal{M}(1)} \quad (3.6)$$

is the mean value of u^n (and u^{n+1} , since the baseline methods conserve the total mass due to its linearity).

For the NLS equation, both the total mass \mathcal{M} and the total momentum \mathcal{P} are quadratic invariants. Since even the projection onto an ellipsoid is not completely straightforward (since it involves solving a quartic equation, for which no simple closed-form solution exists), we use a simplified projection method using the gradient of the momentum at the current solution $u^n = v^n + iw^n$. This leads to the ansatz

$$\pi \begin{pmatrix} v \\ w \end{pmatrix} = \lambda \begin{pmatrix} v \\ w \end{pmatrix} + \mu \begin{pmatrix} w_x \\ -v_x \end{pmatrix} \quad (3.7)$$

for Lagrange multipliers $\lambda, \mu \in \mathbb{R}$ such that

$$\mathcal{M}(\pi(u)) = \mathcal{M}(u^n) \quad \text{and} \quad \mathcal{P}(\pi(u)) = \mathcal{P}(u^n). \quad (3.8)$$

The condition on the total mass can be written as

$$\begin{aligned} \mathcal{M}(u^n) = \mathcal{M}(\pi(u)) &= \int ((\lambda v + \mu w_x)^2 + (\lambda w - \mu v_x)^2) \\ &= \lambda^2 \int (v^2 + w^2) + 2\lambda\mu \int (vw_x - wv_x) + \mu^2 \int (v_x^2 + w_x^2) \\ &= \lambda^2 \mathcal{M}(v, w) + 2\lambda\mu \mathcal{P}(v, w) + \mu^2 \mathcal{M}(v_x, w_x). \end{aligned} \quad (3.9)$$

The condition on the total momentum can be written as

$$\begin{aligned} \mathcal{P}(u^n) = \mathcal{P}(\pi(u)) &= 2 \int (\lambda v + \mu w_x)(\lambda w_x - \mu v_{xx}) \\ &= 2\lambda^2 \int vw_x + 2\lambda\mu \int (v_x^2 + w_x^2) + 2\mu^2 \int v_x w_{xx} \\ &= \lambda^2 \mathcal{P}(v, w) + 2\lambda\mu \mathcal{M}(v_x, w_x) + \mu^2 \mathcal{P}(v_x, w_x). \end{aligned} \quad (3.10)$$

For given (v, w) , the conditions (3.9) and (3.10) form a system of two quadratic equations for the two unknowns λ and μ . We solve this system using Newton's method implemented in SimpleNonlinearSolve.jl [72] with initial guess $\lambda = 1$ and $\mu = 0$.

3.2 Numerical verification of the fully-discrete invariant conservation

We verify the conservation of the mass, momentum, and energy for the fully discrete schemes using the same two-wave setups as in Section 2.5.

We choose $N = 2^8$ nodes in space and use the fifth-order ARK method of [52] as the baseline time integration method. Compared to Section 2.5, we choose bigger time step sizes Δt such that the error in time is not negligible anymore. We choose final times such that the baseline method performs 10^4 time steps for each equation.

The results shown in Figure 2 confirm the theoretical predictions. In particular, relaxation methods constructed to conserve the total mass and energy (only) conserve these invariants but not the total momentum³. The new quadratic-preserving relaxation methods using the projection operators to conserve the total mass and momentum conserve all three invariants up to machine precision.

For a single solitary wave, conserving the total mass and energy typically leads to very good results. In particular, it results in a linear error growth in time (if the spatial error is negligible) instead of a quadratic error growth for general time integration methods [10, 28, 35]. Here, we

³For the BBM and KdV equations, these are the standard relaxation methods that conserve all linear invariants automatically; for the NLS equation, this is the quadratic-preserving relaxation method of [77] without the modification to conserve the momentum.

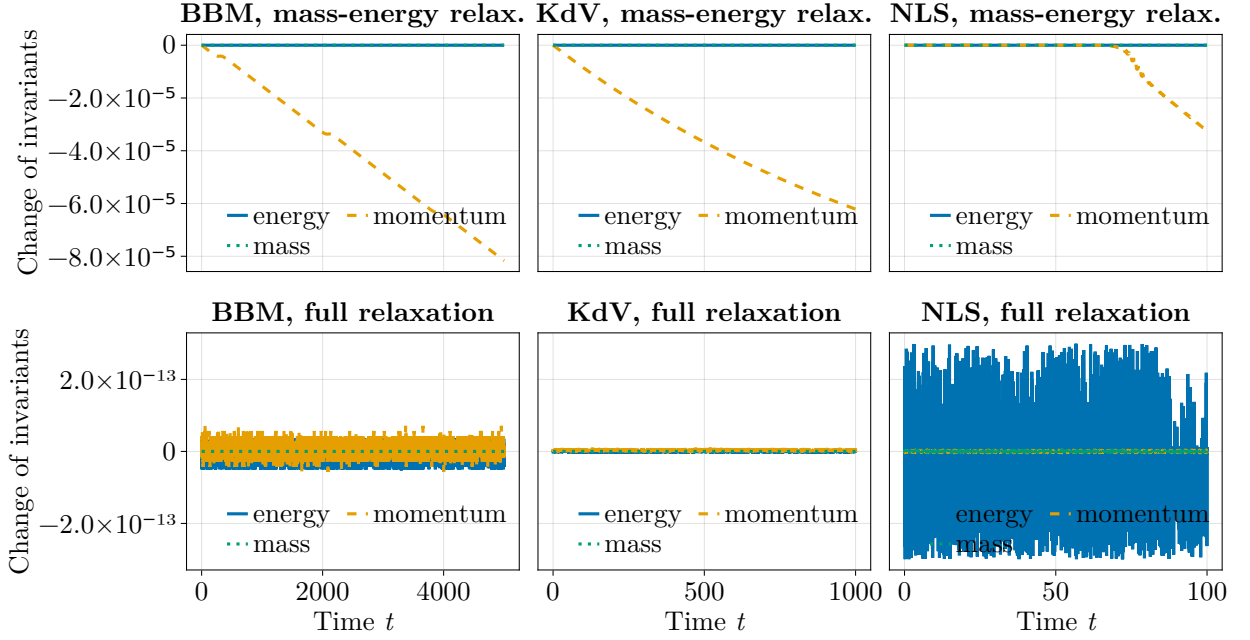


Figure 2: Change of invariants over time for the Fourier Galerkin semidiscretizations of the BBM, KdV, and NLS equations with two interacting solitary waves for two versions of relaxation. The time integration is performed with the fifth-order method of [52] with $\Delta t = 0.5$ for the BBM, $\Delta t = 0.1$ for the KdV, and $\Delta t = 0.01$ for the NLS equation.

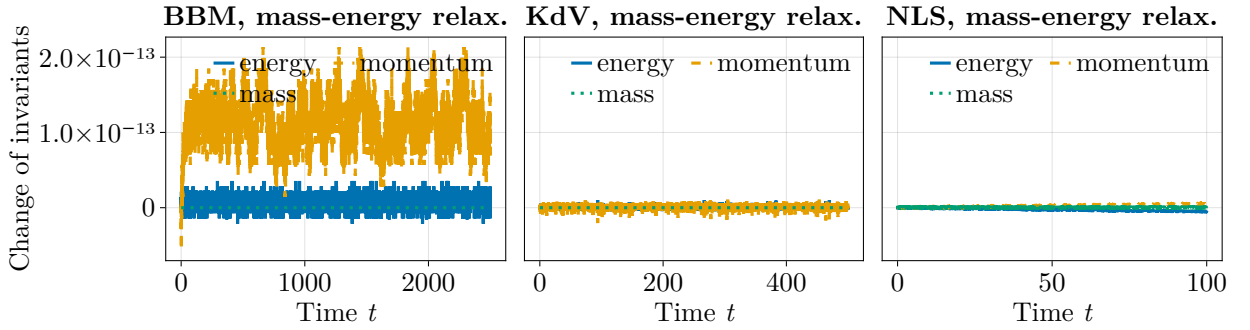


Figure 3: Change of invariants over time for the Fourier Galerkin semidiscretizations of the BBM, KdV, and NLS equations with one solitary wave with relaxation to enforce conservation of the total mass and energy. The time integration is performed with the fourth-order method of [52] with $\Delta t = 0.25$ for the BBM, $\Delta t = 0.05$ for the KdV, and $\Delta t = 0.01$ for the NLS equation.

choose the solitary wave with the larger wave speed from the two-wave setup for the BBM and KdV equations as well as the single-soliton solution used in [18, 77] for the NLS equation.

The results shown in Figure 3 demonstrate that even the mass- and energy-conserving relaxation methods lead to conservation of the momentum up to small oscillations close to machine accuracy. Please note that this is a special property when integrating a single solitary wave and does not hold in more general cases such as the two-wave setups considered before.

4 Error growth for multiple-soliton solutions

We measure the error growth in time for the two-soliton solutions of the KdV and NLS equations described in Section 2.5. Moreover, we consider the three-soliton solution [47, 48]

$$\begin{aligned} u &= 12 \partial_x^2 \log F, \\ F &= 1 + e^{\eta_1} + e^{\eta_2} + e^{\eta_3} + a_{12} e^{\eta_1 + \eta_2} + a_{13} e^{\eta_1 + \eta_3} + a_{23} e^{\eta_2 + \eta_3} + a_{12} a_{13} a_{23} e^{\eta_1 + \eta_2 + \eta_3}, \\ \eta_i &= k_i(x - x_{i,0}) - k_i^3 t, \end{aligned} \quad (4.1)$$

of the KdV equation with parameters

$$k_1 = 0.75, \quad k_2 = 0.5, \quad k_3 = 0.25, \quad x_{1,0} = -100, \quad x_{2,0} = 0, \quad x_{3,0} = 100, \quad (4.2)$$

and the spatial domain $[-400, 400]$ with periodic boundary conditions. The time span $[0, 1500]$ ensures that the waves interact. We use Enzyme.jl [68, 69] to compute the second-derivative via automatic/algebraic differentiation (AD). Since we use a domain twice as large as for the two-soliton solution, we double the number of nodes accordingly ($N = 2^{10}$ for two solitons, $N = 2^{11}$ for three solitons) to obtain comparable spatial errors.

For the NLS equation (1.5), we use the three-soliton solution used in [18] with $N = 2^{10}$ nodes in the spatial domain $[-35, 35]$.

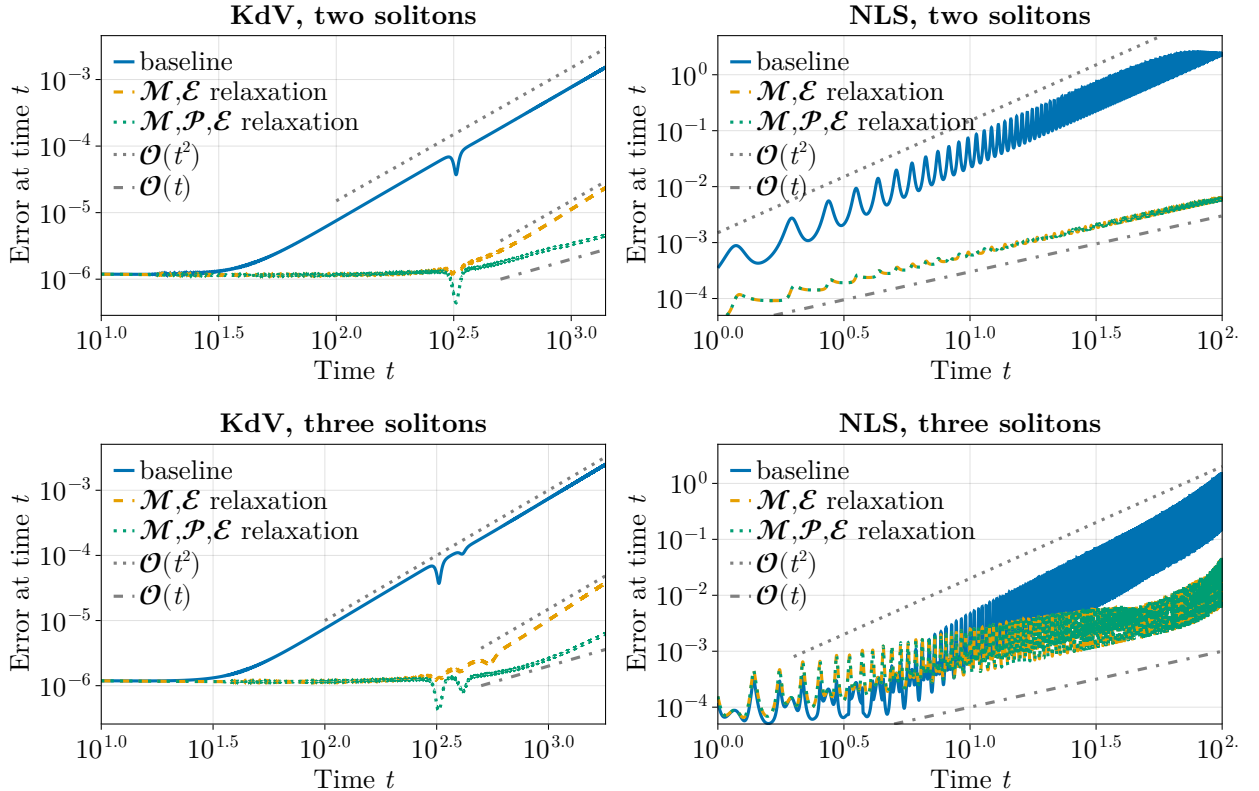


Figure 4: Error growth in time for two- and three-soliton solutions of the KdV and NLS equations discretized using Fourier Galerkin methods in space. The time integration is performed with the fifth-order method of [52] with $\Delta t = 0.1$ for the KdV equation as well as $\Delta t = 0.01$ (two solitons) and $\Delta t = 0.001$ (three solitons) for the NLS equation.

The results are shown in Figure 4. For the KdV equation, the interaction time of two solitons can be seen clearly in the error growth plot (the small bumps, e.g., around $t = 10^{2.5}$). As expected, the error of the baseline method grows quadratically in time. Before the first soliton interaction, the

relaxation methods conserving either the mass and energy or all three invariants behave similarly well. However, after the interaction, the method conserving only two invariants has a quadratically growing error while the method conserving all three invariants has a linearly growing error in time. These results are in accordance with the theoretical predictions for two solitons [8]. However, they appear to be better than expected for three solitons.

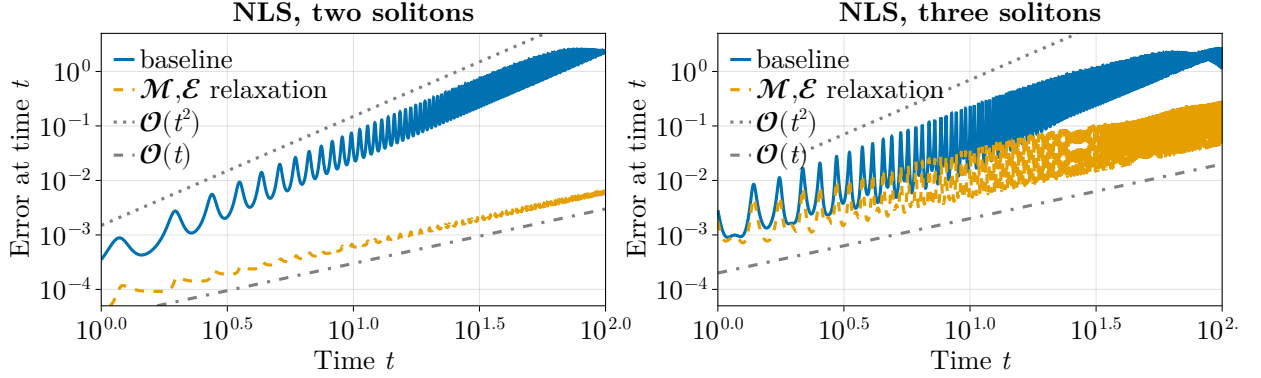


Figure 5: Error growth in time for two- and three-soliton solutions of the NLS equation discretized using Fourier collocation methods in space. The time integration is performed with the fifth-order method of [52] with $\Delta t = 0.01$ (two solitons) and $\Delta t = 0.002$ (three solitons).

The numerical methods behave differently for the NLS equation. In accordance with the numerical results of [77] for two solitons, we observe quadratic error growth in time for the baseline method and a linear error growth for the mass- and energy-conserving method. However, conserving the momentum in addition does not improve the results further. For three solitons, conserving the momentum does also not improve the results further. Moreover, both relaxation methods result in an eventually quadratic error growth, in contrast to the numerical results shown in [77] obtained using a Fourier collocation method in space that conserves only the mass and energy. The corresponding results are shown in Figure 5.

4.1 Fourier collocation versus Galerkin methods for NLS

To investigate the issue further, we compare the change of the invariants over time for the three-soliton solutions of the NLS equation using Fourier Galerkin and collocation methods in space; the results are shown in Figure 6. We clearly observe that the momentum is much better conserved for the collocation method with mass-energy relaxation, although there are no theoretical guarantees for this. This indicates that other properties like symmetry properties may play a role here and result in the improved error growth of the collocation method.

Next, we consider the defocusing NLS equation with $\beta = -1$ and gray/dark soliton solutions. Specifically, we use the one-gray-soliton solution

$$u(t, x) = \sqrt{b_0} e^{i(\kappa(x-ct)-\omega t)} \left(i \sqrt{\frac{b_1}{b_0}} + \sqrt{1 - \frac{b_1}{b_0}} \tanh \left(\sqrt{\frac{b_0 - b_1}{2}} (x - ct) \right) \right) \quad (4.3)$$

with background mass density $b_0 = 1.5$, minimal mass density $b_1 = 1$, speed $c = 2\sqrt{2}$, and derived parameters

$$\kappa = \frac{c - \sqrt{2b_1}}{2}, \quad \omega = b_0 - \frac{c^2 - 2b_1}{4}, \quad (4.4)$$

see, e.g., [5]. This moving gray soliton decays to a background with constant rate of change of the phase so that the total momentum is not zero. We computed the domain boundaries

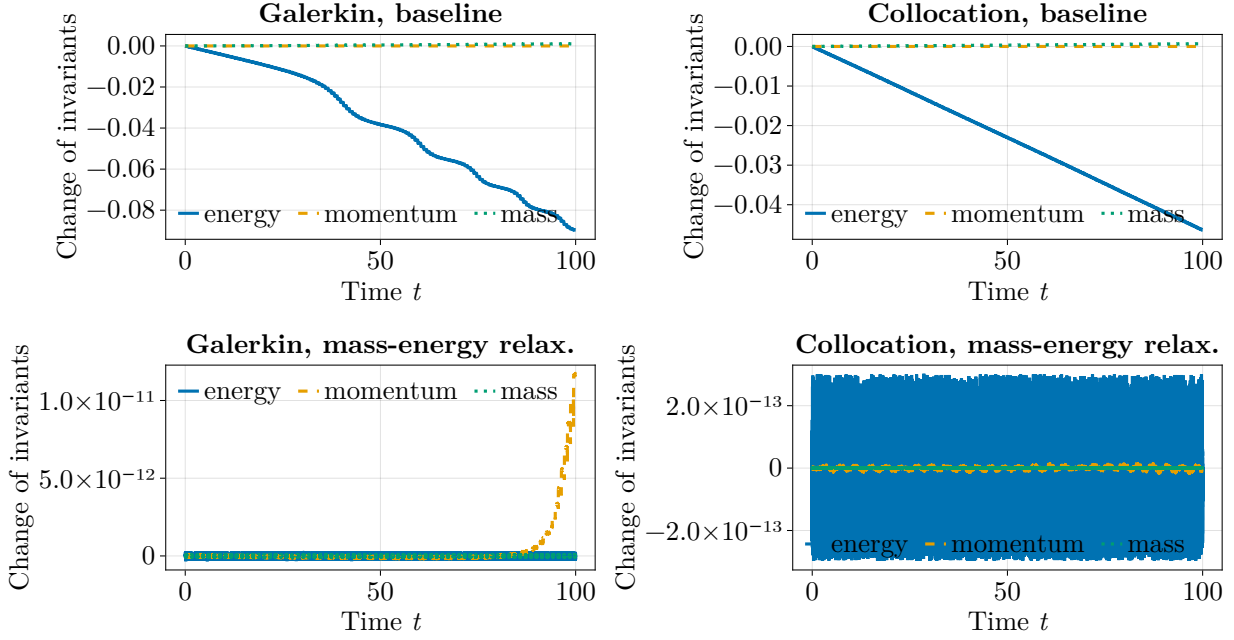


Figure 6: Change of invariants for the three-soliton solution of the NLS equation discretized using Fourier Galerkin and collocation methods in space. The time integration is performed with the fifth-order method of [52] with $\Delta t = 0.002$.

± 31.970600318475647 such that the gray soliton is periodic (up to machine precision) and use 2^8 nodes for the spatial semidiscretization.

Moreover, we consider the (moving) two-gray-soliton solution

$$u(t, x) = e^{i(kx - k^2 t)} \tilde{u}(t, x - 2kt), \quad k = 2, \quad (4.5)$$

where

$$\tilde{u}(t, x) = e^{-ia_3 t} \frac{(2a_3 - 4a_1) \cosh(\mu t/2) - 2\sqrt{a_1 a_3} \cosh(2px/\sqrt{2}) - i\mu \sinh(\mu t/2)}{2\sqrt{a_3} \cosh(\mu t/2) + 2\sqrt{a_1} \cosh(2px/\sqrt{2})} \quad (4.6)$$

describes two colliding gray solitons in a steady reference frame [5] with background mass density $a_3 = 1.5$, minimum mass density $a_1 = 1$, and derived parameters

$$\mu = 4\sqrt{a_1(a_3 - a_1)}, \quad p = \sqrt{a_3 - a_1}. \quad (4.7)$$

Since the two solitons collide at $t = 0$, we choose the time span $[-70, 70]$. The spatial domain boundaries ± 409.97784129346803 are chosen such that the background is periodic (up to machine precision). We use 2^{11} nodes for the spatial semidiscretization.

The error growth in time for these gray soliton solutions is shown in Figure 7. As expected, the baseline scheme has a quadratic error growth for all cases. For one gray soliton, both spatial discretizations (Galerkin and collocation) with relaxation (only mass and energy for collocation; also momentum for Galerkin) result in a linear error growth in time. For two gray solitons, we observe that the mass-, momentum-, and energy-conserving Fourier Galerkin method with relaxation has a linear error growth while the mass- and energy-conserving methods have a quadratically growing error. Thus, the additional conservation of the momentum improves the long-time accuracy, but increases the error for shorter times a bit.

These results differ from the previous findings for the three-soliton solution of the focusing NLS equation. This is related to the conservation properties of the relaxation methods enforcing only the mass and energy. For a moving background, the momentum is essentially conserved for the

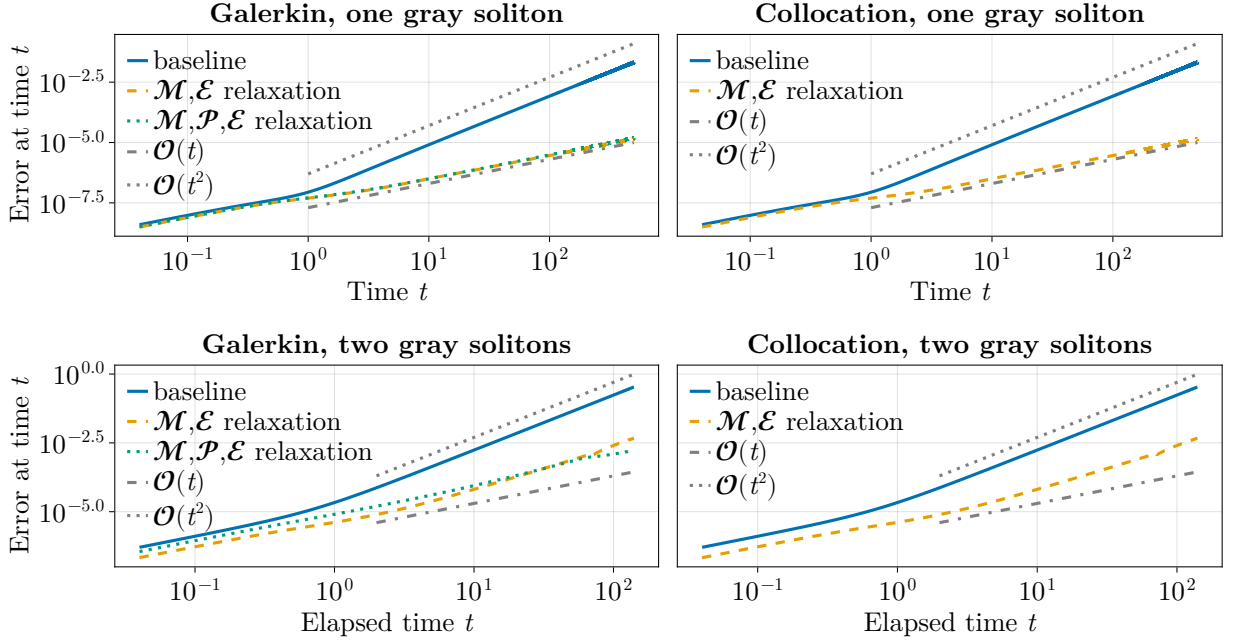


Figure 7: Error growth in time for moving one- and two-gray-soliton solutions of the NLS equation. The time integration is performed with the fifth-order method of [52] with $\Delta t = 0.04$. The two solitons collide after an elapsed time of about $t = 70$.

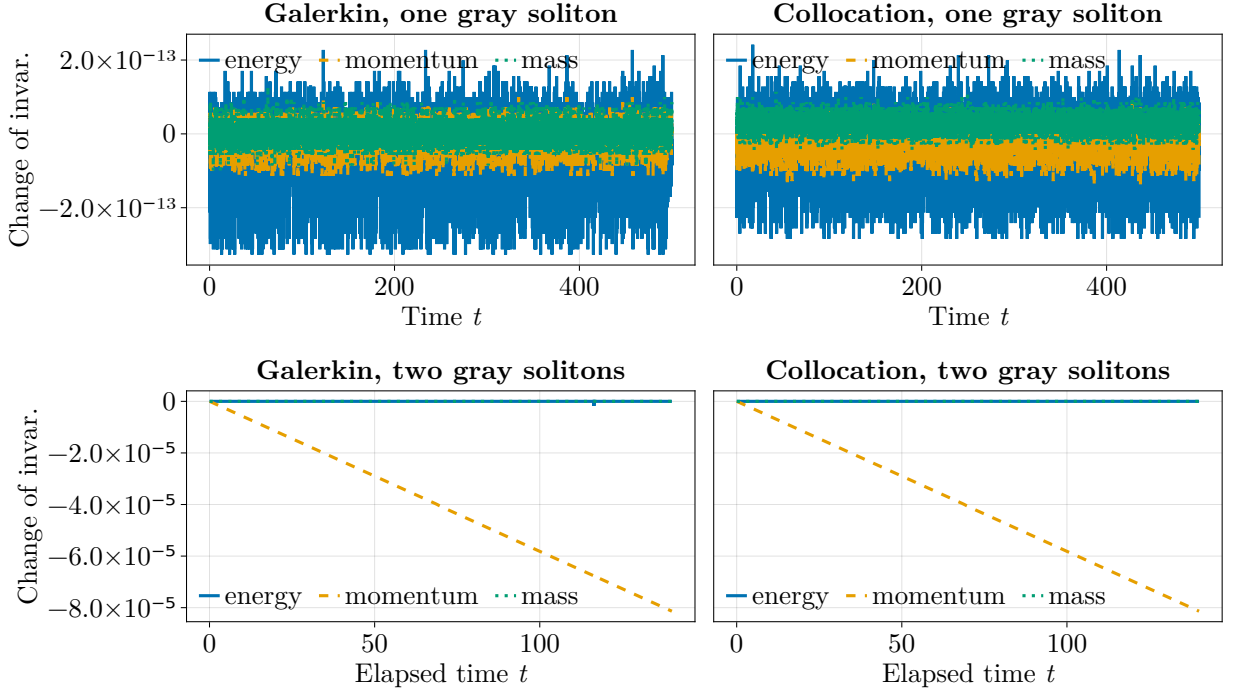


Figure 8: Change of invariants for moving one- and two-gray-soliton solutions of the NLS equation with mass- and energy-conserving relaxation. The time integration is performed with the fifth-order method of [52] with $\Delta t = 0.04$.

one-soliton solution (although this is not guaranteed by relaxation). However, the momentum varies clearly for the two solitons if relaxation is used to conserve only the mass and energy, see Figure 8.

5 Performance comparisons

In this section we compare the computational performance of the methods proposed here with some previous methods from the literature. First, we can compare the present method with the scheme we proposed previously for the NLS equation (that scheme conserves only mass and energy, not momentum). For both spatial discretizations (Fourier Galerkin here and Fourier collocation there), the most costly part is the FFT required to switch between nodal and modal space with complexity $O(M \log M)$ for M nodes. Since the NLS has a cubic nonlinearity, we need $M > 2N$ for a Galerkin method while we only need $M = N$ for a Fourier collocation method (conserving mass and energy [77]). To compute the energy with quartic nonlinearity (e.g., to apply relaxation or projection to conserve the energy), we even require $M > 3N/2$ for the Galerkin method. Thus, the Fourier Galerkin method is typically (at least) twice as expensive as the Fourier collocation method for the same number of degrees of freedom.

For the existing schemes that conserve all three of mass, momentum, and energy, unfortunately no code is publicly available [6, 98]. Instead, we compare with two methods that conserve just two quantities and for which code is available. All tests were performed on a workstation with two sockets of 20 dual-threaded Intel Xeon Gold 6230 CPUs running Ubuntu 22.04.

The method of Andrews & Farrell [9] conserves mass and energy for BBM. We apply their implementation and ours to the problem presented in Section 4.2.1 of that work. Namely, we solve the BBM equation on the domain $x \in [-50, 50]$ with periodic boundary conditions and initial condition

$$u(x, t = 0) = \frac{3\sqrt{5} - 3}{2} \operatorname{sech} \left(\frac{\sqrt{5} - 1}{4} x \right)^2. \quad (5.1)$$

We solve up to time $t = 2 \times 10^4$, and use a mesh with 100 degrees for both methods. The method proposed here runs in about 0.40 seconds while that of Andrews & Farrell runs in 1141 seconds.

Finally, we also compare with the code of Bai et al. [12], which conserves mass and energy for the NLS equation. We consider the one-soliton problem from Section 4 of that work, given by

$$u(x, t) = \operatorname{sech}(x + 4t) \exp(-i(2x + 3t)).$$

We solve the problem on the domain $x \in [-40, 40]$ for $0 \leq t \leq 1$ and measure the L^2 norm of the error at the final time. Using the same discretization considered in Figure 4.4(b) of that work the wall clock time for a run using $\Delta t = 1/512$ and 1024 points in space is approximately 90 seconds and results in an error of 1.26×10^{-6} . We previously compared our mass- and energy-conserving Fourier collocation methods with relaxation to their methods in [77], and found that our methods were orders of magnitude faster and significantly more accurate. Since Fourier Galerkin methods are roughly twice as expensive as the Fourier collocation methods used in [77], they are still orders of magnitude faster than the methods of [12]. Specifically, the Fourier collocation code runs in 0.17 seconds, the Fourier Galerkin code runs in 0.36 seconds, and the code of Bai et al. runs in 90 seconds. The codes proposed here yield errors of 10^{-11} or less, while that of Bai et al. yields an error of 1.26×10^{-6} .

6 Hyperbolic approximation of the nonlinear Schrödinger equation

We extend the structure-preserving methods to a hyperbolic approximation of the NLS equation. There are two such hyperbolizations conserving (appropriate approximations of) the mass, momentum, and energy. The first one is based on the hydrodynamic formulation and is thus mostly useful for the defocusing case without vacuum [32]; it conserves the mass and momentum as linear invariants and the energy as nonlinear invariant. Thus, classical relaxation in time [80, 83] can be used to conserve all three invariants. Here, we focus on the second hyperbolization [17] conserving

all three invariants with a structure similar to the original NLS equation. This hyperbolization does not require the absence of vacuum. It is given by [17]

$$\begin{aligned} iq_t^0 + q_x^1 &= -\beta|q^0|^2 q^0, \\ i\tau q_t^1 - q_x^0 &= -q^1, \end{aligned} \quad (6.1)$$

where $\tau > 0$ is a relaxation parameter; as $\tau \rightarrow 0$, the solution q^0 of the hyperbolization (6.1) converges formally to the original NLS equation (1.5). Introducing the real and imaginary parts $q^0 = v + iw$ and $q^1 = \nu + i\omega$ as in [77], we obtain

$$\begin{aligned} v_t &= -\omega_x - \beta(v^2 + w^2)w, \\ w_t &= \nu_x + \beta(v^2 + w^2)v, \\ \tau v_t &= w_x - \omega, \\ \tau \omega_t &= -v_x + \nu. \end{aligned} \quad (6.2)$$

Using this formulation, the invariants of (6.1) [17] can be written as

$$\begin{aligned} \mathcal{M} &= \int (v^2 + w^2 + \tau v^2 + \tau \omega^2) dx, \\ \mathcal{P} &= \int (vw_x - v_x w + \tau v \omega_x - \tau v_x \omega) dx = 2 \int (vw_x + \tau v \omega_x) dx, \\ \mathcal{E} &= \int \left(2v v_x - v^2 + 2\omega w_x - \omega^2 - \frac{\beta}{2}(v^2 + w^2)^2 \right) dx. \end{aligned} \quad (6.3)$$

A Fourier collocation semidiscretization of (6.2) conserving the mass and energy has been developed in [77]. Here, we consider the Fourier Galerkin semidiscretization

$$\begin{aligned} v_t &= -\omega_x - \beta P(v^2 + w^2)w, \\ w_t &= \nu_x + \beta P(v^2 + w^2)v, \\ \tau v_t &= w_x - \omega, \\ \tau \omega_t &= -v_x + \nu. \end{aligned} \quad (6.4)$$

Theorem 6.1. *The Fourier Galerkin semidiscretization (6.4) of the hyperbolic NLS equation (6.2) conserves the total mass, momentum, and energy (6.3).*

Proof. The total mass is conserved since

$$\begin{aligned} \partial_t \mathcal{M} &= 2\langle v, v_t \rangle + 2\langle w, w_t \rangle + 2\langle \nu, \tau v_t \rangle + 2\langle \omega, \tau \omega_t \rangle \\ &= 2\langle v, -\omega_x - \beta P(v^2 + w^2)w \rangle + 2\langle w, \nu_x + \beta P(v^2 + w^2)v \rangle \\ &\quad + 2\langle \nu, w_x - \omega \rangle + 2\langle \omega, -v_x + \nu \rangle \\ &= -2\beta \int (v^2 + w^2)(vw - wv) dx = 0. \end{aligned} \quad (6.5)$$

Similarly, the total momentum is conserved since

$$\begin{aligned} \partial_t \mathcal{P} &= 2\langle w_x, v_t \rangle - 2\langle v_x, w_t \rangle + 2\langle \omega_x, \tau v_t \rangle - 2\langle \nu_x, \tau \omega_t \rangle \\ &= 2\langle w_x, -\omega_x - \beta P(v^2 + w^2)w \rangle - 2\langle v_x, \nu_x + \beta P(v^2 + w^2)v \rangle \\ &\quad + 2\langle \omega_x, w_x - \omega \rangle - 2\langle \nu_x, -v_x + \nu \rangle \\ &= -2\beta \int (v^2 + w^2)(ww_x + vv_x) dx = -\beta \int (v^2 + w^2)_x^2 dx = 0. \end{aligned} \quad (6.6)$$

Finally, the total energy is conserved since

$$\begin{aligned}
\partial_t \mathcal{E} &= -2\langle v_x, v_t \rangle - 2\beta\langle (v^2 + w^2)v, v_t \rangle - 2\langle \omega_x, w_t \rangle - 2\beta\langle (v^2 + w^2)w, w_t \rangle \\
&\quad + 2\langle v_x, v_t \rangle - 2\langle v, v_t \rangle + 2\langle w_x, \omega_t \rangle - 2\langle \omega, \omega_t \rangle \\
&= -2\langle v_x, -\omega_x - \beta P(v^2 + w^2)w \rangle - 2\beta\langle (v^2 + w^2)v, -\omega_x - \beta P(v^2 + w^2)w \rangle \\
&\quad - 2\langle \omega_x, v_x + \beta P(v^2 + w^2)v \rangle - 2\beta\langle (v^2 + w^2)w, v_x + \beta P(v^2 + w^2)v \rangle \\
&\quad + 2\tau^{-1}\langle v_x, w_x - \omega \rangle - 2\tau^{-1}\langle v, w_x - \omega \rangle \\
&\quad + 2\tau^{-1}\langle w_x, -v_x + v \rangle - 2\tau^{-1}\langle \omega, -v_x + v \rangle = 0.
\end{aligned} \tag{6.7}$$

As before, we used the exactness of the L^2 projection P for these computations. \square

To apply mass- and energy-conserving relaxation methods, we use the simplified projection method to conserve the total mass described in [77], i.e., we scale v, w by α_1 and v, ω by α_2 , where

$$\begin{aligned}
\alpha_1 &= \frac{p^2(\tau - 1)\tau^2 + \sqrt{-p^2q^2(\tau - 1)^2\tau + c(q^2 + p^2\tau^3)}}{q^2 + p^2\tau^3}, \\
\alpha_2 &= \frac{q^2(1 - \tau) + \tau\sqrt{-p^2q^2(\tau - 1)^2\tau + c(q^2 + p^2\tau^3)}}{q^2 + p^2\tau^3},
\end{aligned} \tag{6.8}$$

c is the desired value of the mass (6.3), and

$$q^2 = \|v\|_{L^2}^2 + \|w\|_{L^2}^2, \quad p^2 = \|v\|_{L^2}^2 + \|\omega\|_{L^2}^2. \tag{6.9}$$

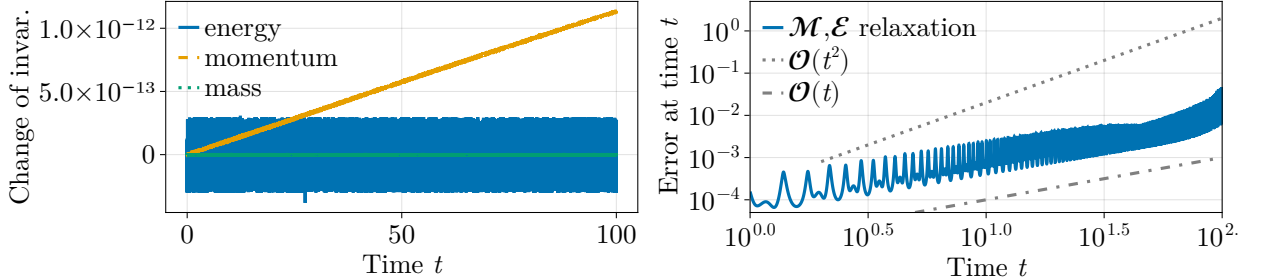


Figure 9: Numerical results for the hyperbolized NLS equation with $\tau = 10^{-9}$ initialized with the three-soliton solution of the NLS equation, which is used to compute the error. The time integration is performed with the fifth-order method of [52] with $\Delta t = 0.001$ and mass- and energy-conserving relaxation.

The hyperbolization behaves similarly to the original NLS equation. Thus, we only show a subset of numerical results. Figure 9 demonstrates that the results agree very well with the original NLS equation for $\tau = 10^{-9}$. In particular, we observe an error growth behavior similar to Figure 4; mass and energy are conserved as expected, and the momentum grows slightly (since it is not enforced to be constant by relaxation here).

7 Conclusions and future directions

The schemes we have proposed are capable of preserving mass, momentum, and energy to machine precision, while also running faster (by orders of magnitude) than other recently-proposed schemes that conserve only two of these quantities. Furthermore, they can be of arbitrarily high order, simply

by using sufficiently high order Runge-Kutta methods in time. Their performance advantage over implicit methods is due to the fact that they only require the solution of a scalar algebraic equation at each step.

For the numerical solution of integrable systems, it is natural to ask whether similar schemes could be designed to conserve even more invariants. This seems difficult in terms of both the spatial and temporal discretization. We have found that Fourier Galerkin methods do not preserve, for instance, the fourth invariant of KdV. Meanwhile, the efficiency of our projection-based relaxation method relies crucially on the efficiency of the inner projection onto the manifolds defined by the first invariants. While the idea can be extended directly to projections that conserve N invariants (with relaxation to conserve invariant $N + 1$), efficiency will likely be significantly reduced if the inner projections are too expensive. The Toda lattice and the Ablowitz-Ladik lattice are natural systems on which to test time discretizations that may preserve several invariants.

While our description and experiments have been restricted to one spatial dimension, the schemes can be extended in a natural way to higher dimensions. In order to conserve momentum, we require the imposition of periodic boundary conditions. With more general boundary conditions, mass and energy are still conserved, but we note that conservation of mass and energy can be achieved also with other SBP spatial discretizations along with previously-published time discretization approaches. Another natural question is whether the effort to conserve three invariants is worthwhile. Of course, conservation is already highly desirable from a physical point of view, and our experiments show that in some cases conserving all three quantities gives a significant quantitative advantage over conserving just two, with respect to long-time error growth. The downside of imposing all three discrete conservation laws is that one must use Fourier Galerkin methods, which cost notably more than collocation methods. A more detailed comparison of the cost of different conservation techniques (especially with respect to time) is the subject of future work.

Acknowledgments

HR was supported by the Deutsche Forschungsgemeinschaft (DFG, German Research Foundation, project numbers 513301895 and 528753982 as well as within the DFG priority program SPP 2410 with project number 526031774). DK was supported by funding from King Abdullah University of Science and Technology.

We thank Mario Ricchiutto for hosting us in Bordeaux during the week October 6–10 2025, where this project was initiated in breakfast discussions.

References

- [1] R. Abgrall. “A general framework to construct schemes satisfying additional conservation relations. Application to entropy conservative and entropy dissipative schemes.” In: *Journal of Computational Physics* 372 (2018), pp. 640–666. doi: [10.1016/j.jcp.2018.06.031](https://doi.org/10.1016/j.jcp.2018.06.031). arXiv: [1711.10358](https://arxiv.org/abs/1711.10358) [math.NA].
- [2] R. Abgrall, E. L. Mélédo, P. Öffner, and D. Torlo. “Relaxation Deferred Correction Methods and their Applications to Residual Distribution Schemes.” In: *The SMAI Journal of Computational Mathematics* 8 (2022), pp. 125–160. doi: [10.5802/smai-jcm.82](https://doi.org/10.5802/smai-jcm.82). arXiv: [2106.05005](https://arxiv.org/abs/2106.05005) [math.NA].
- [3] R. Abgrall, P. Öffner, and H. Ranocha. “Reinterpretation and Extension of Entropy Correction Terms for Residual Distribution and Discontinuous Galerkin Schemes: Application to Structure Preserving Discretization.” In: *Journal of Computational Physics* 453 (Mar. 2022), p. 110955. doi: [10.1016/j.jcp.2022.110955](https://doi.org/10.1016/j.jcp.2022.110955). arXiv: [1908.04556](https://arxiv.org/abs/1908.04556) [math.NA].

[4] M. J. Ablowitz, B. Prinari, and A. D. Trubatch. *Discrete and continuous nonlinear Schrödinger systems*. Vol. 302. Cambridge University Press, 2004. doi: [10.1017/CBO9780511546709](https://doi.org/10.1017/CBO9780511546709).

[5] N. Akhmediev and A. Ankiewicz. “First-order exact solutions of the nonlinear Schrödinger equation in the normal-dispersion regime.” In: *Physical Review A* 47.4 (1993), p. 3213. doi: [10.1103/PhysRevA.47.3213](https://doi.org/10.1103/PhysRevA.47.3213).

[6] G. Akrivis, B. Li, R. Tang, and H. Zhang. “High-order mass-, energy-and momentum-conserving methods for the nonlinear Schrödinger equation.” In: *Journal of Computational Physics* 532 (2025), p. 113974. doi: [10.1016/j.jcp.2025.113974](https://doi.org/10.1016/j.jcp.2025.113974).

[7] G. D. Akrivis, V. A. Dougalis, and O. A. Karakashian. “On fully discrete Galerkin methods of second-order temporal accuracy for the nonlinear Schrödinger equation.” In: *Numerische Mathematik* 59.1 (1991), pp. 31–53. doi: [10.1007/BF01385769](https://doi.org/10.1007/BF01385769).

[8] J. Álvarez and A. Durán. “Error propagation when approximating multi-solitons: The KdV equation as a case study.” In: *Applied Mathematics and Computation* 217.4 (2010), pp. 1522–1539. doi: [10.1016/j.amc.2009.06.033](https://doi.org/10.1016/j.amc.2009.06.033).

[9] B. D. Andrews and P. E. Farrell. *Conservative and dissipative discretisations of multi-conservative ODEs and GENERIC systems*. Nov. 2025. arXiv: [2511.23266](https://arxiv.org/abs/2511.23266) [math.NA].

[10] A Araújo and A. Durán. “Error propagation in the numerical integration of solitary waves. The regularized long wave equation.” In: *Applied Numerical Mathematics* 36.2-3 (2001), pp. 197–217. doi: [10.1016/S0168-9274\(99\)00148-8](https://doi.org/10.1016/S0168-9274(99)00148-8).

[11] U. M. Ascher, S. J. Ruuth, and R. J. Spiteri. “Implicit-explicit Runge-Kutta methods for time-dependent partial differential equations.” In: *Applied Numerical Mathematics* 25.2-3 (1997), pp. 151–167. doi: [10.1016/S0168-9274\(97\)00056-1](https://doi.org/10.1016/S0168-9274(97)00056-1).

[12] G. Bai, J. Hu, and B. Li. “High-order mass-and energy-conserving methods for the nonlinear Schrödinger equation.” In: *SIAM Journal on Scientific Computing* 46.2 (2024), A1026–A1046. doi: [10.1137/22M152178X](https://doi.org/10.1137/22M152178X).

[13] T. B. Benjamin, J. L. Bona, and J. J. Mahony. “Model equations for long waves in nonlinear dispersive systems.” In: *Philosophical Transactions of the Royal Society of London. Series A, Mathematical and Physical Sciences* 272.1220 (1972), pp. 47–78. doi: [10.1098/rsta.1972.0032](https://doi.org/10.1098/rsta.1972.0032).

[14] C. Besse. “A relaxation scheme for the nonlinear Schrödinger equation.” In: *SIAM Journal on Numerical Analysis* 42.3 (2004), pp. 934–952. doi: [10.1137/S0036142901396521](https://doi.org/10.1137/S0036142901396521).

[15] C. Besse, S. Descombes, G. Dujardin, and I. Lacroix-Violet. “Energy-preserving methods for nonlinear Schrödinger equations.” In: *IMA Journal of Numerical Analysis* 41.1 (2021), pp. 618–653. doi: [10.1093/imanum/drz067](https://doi.org/10.1093/imanum/drz067).

[16] J. Bezanson, A. Edelman, S. Karpinski, and V. B. Shah. “Julia: A Fresh Approach to Numerical Computing.” In: *SIAM Review* 59.1 (2017), pp. 65–98. doi: [10.1137/141000671](https://doi.org/10.1137/141000671). arXiv: [1411.1607](https://arxiv.org/abs/1411.1607) [cs.MS].

[17] A. Biswas, L. S. Busaleh, D. I. Ketcheson, C. Muñoz-Moncayo, and M. Rajvanshi. *A Hyperbolic Approximation of the Nonlinear Schrödinger Equation*. 2025. arXiv: [2505.21424](https://arxiv.org/abs/2505.21424) [math.AP].

[18] A. Biswas and D. I. Ketcheson. “Accurate Solution of the Nonlinear Schrödinger Equation via Conservative Multiple-Relaxation ImEx Methods.” In: *SIAM Journal of Scientific Computing* 46.6 (2024), A3827–A3848. doi: [10.1137/23M1598118](https://doi.org/10.1137/23M1598118). arXiv: [2309.02324](https://arxiv.org/abs/2309.02324) [math.NA].

[19] A. Biswas and D. I. Ketcheson. “Multiple-relaxation Runge Kutta methods for conservative dynamical systems.” In: *Journal of Scientific Computing* 97.1 (2023), p. 4. doi: [10.1007/s10915-023-02312-4](https://doi.org/10.1007/s10915-023-02312-4).

[20] A. Biswas, D. I. Ketcheson, H. Ranocha, and J. Schütz. “Traveling-wave solutions and structure-preserving numerical methods for a hyperbolic approximation of the Korteweg-de Vries equation.” In: *Journal of Scientific Computing* 103 (May 2025), p. 90. doi: [10.1007/s10915-025-02898-x](https://doi.org/10.1007/s10915-025-02898-x). arXiv: [2412.17117](https://arxiv.org/abs/2412.17117) [math.NA].

[21] S. Bleecke, A. Biswas, D. I. Ketcheson, J. Schütz, and H. Ranocha. *Asymptotic-preserving and energy-conserving methods for a hyperbolic approximation of the BBM equation*. Nov. 2025. arXiv: 2511.10044 [math.NA].

[22] M. Calvo, M. Laburta, J. I. Montijano, and L. Rández. “Projection methods preserving Lyapunov functions.” In: *BIT Numerical Mathematics* 50.2 (2010), pp. 223–241. doi: 10.1007/s10543-010-0259-3.

[23] B. Cano. “Conserved quantities of some Hamiltonian wave equations after full discretization.” In: *Numerische Mathematik* 103.2 (2006), pp. 197–223. doi: 10.1007/s00211-006-0680-3.

[24] E. Celledoni, R. I. McLachlan, D. I. McLaren, B. Owren, G. R. W. Quispel, and W. Wright. “Energy-preserving Runge-Kutta methods.” In: *ESAIM: Mathematical Modelling and Numerical Analysis (M2AN)* 43 (2009), pp. 645–649. doi: 10.1051/m2an/2009020.

[25] Y. Chen, B. Dong, and R. Pereira. “A new conservative discontinuous Galerkin method via implicit penalization for the generalized Korteweg-de Vries equation.” In: *SIAM Journal on Numerical Analysis* 60.6 (2022), pp. 3078–3098. doi: 10.1137/22M1470827.

[26] J. Cui, Z. Xu, Y. Wang, and C. Jiang. “Mass-and energy-preserving exponential Runge-Kutta methods for the nonlinear Schrödinger equation.” In: *Applied Mathematics Letters* 112 (2021), p. 106770. doi: 10.1016/j.aml.2020.106770.

[27] S. Danisch and J. Krumbiegel. “Makie.jl: Flexible high-performance data visualization for Julia.” In: *Journal of Open Source Software* 6.65 (2021), p. 3349. doi: 10.21105/joss.03349.

[28] J De Frutos and J. M. Sanz-Serna. “Accuracy and conservation properties in numerical integration: the case of the Korteweg-de Vries equation.” In: *Numerische Mathematik* 75.4 (1997), pp. 421–445. doi: 10.1007/s002110050247.

[29] K. Dekker and J. G. Verwer. *Stability of Runge-Kutta methods for stiff nonlinear differential equations*. Vol. 2. CWI Monographs. Amsterdam: North-Holland, 1984.

[30] M. Delfour, M. Fortin, and G Payr. “Finite-difference solutions of a non-linear Schrödinger equation.” In: *Journal of computational physics* 44.2 (1981), pp. 277–288. doi: 10.1016/0021-9991(81)90052-8.

[31] S. Derevyanko. “The $(n + 1)/2$ Rule for Dealiasing in the Split-Step Fourier Methods for n -Wave Interactions.” In: *IEEE Photonics Technology Letters* 20.23 (2008), pp. 1929–1931. doi: 10.1109/LPT.2008.2005420.

[32] F. Dhaouadi, N. Favrie, and S. Gavrilyuk. “Extended Lagrangian approach for the defocusing nonlinear Schrödinger equation.” In: *Studies in Applied Mathematics* 142.3 (2019), pp. 336–358. doi: 10.1111/sapm.12238.

[33] D. Doehring, H. Ranocha, and M. Torrilhon. *Paired Explicit Relaxation Runge-Kutta Methods: Entropy-Conservative and Entropy-Stable High-Order Optimized Multirate Time Integration*. July 2025. arXiv: 2507.04991 [math.NA].

[34] V. A. Dougalis and Á. Durán. “A high-order fully discrete scheme for the Korteweg-de Vries equation with a time-stepping procedure of Runge-Kutta-composition type.” In: *IMA Journal of Numerical Analysis* 42.4 (2022), pp. 3022–3057. doi: 10.1093/imanum/drab060.

[35] A. Durán and J. M. Sanz-Serna. “The numerical integration of relative equilibrium solutions. The nonlinear Schrödinger equation.” In: *IMA Journal of Numerical Analysis* 20.2 (2000), pp. 235–261. doi: 10.1093/imanum/20.2.235.

[36] D. C. D. R. Fernández, J. E. Hicken, and D. W. Zingg. “Review of summation-by-parts operators with simultaneous approximation terms for the numerical solution of partial differential equations.” In: *Computers & Fluids* 95 (2014), pp. 171–196. doi: 10.1016/j.compfluid.2014.02.016.

[37] G. Frasca-Caccia and P. E. Hydon. "Numerical preservation of multiple local conservation laws." In: *Applied Mathematics and Computation* 403 (2021), p. 126203. doi: [10.1016/j.amc.2021.126203](https://doi.org/10.1016/j.amc.2021.126203).

[38] G. Frasca-Caccia and P. E. Hydon. "Simple bespoke preservation of two conservation laws." In: *IMA Journal of Numerical Analysis* 40.2 (2020), pp. 1294–1329. doi: [10.1093/imanum/dry087](https://doi.org/10.1093/imanum/dry087).

[39] M. Frigo and S. G. Johnson. "The design and implementation of FFTW3." In: *Proceedings of the IEEE* 93.2 (2005), pp. 216–231. doi: [10.1109/JPROC.2004.840301](https://doi.org/10.1109/JPROC.2004.840301).

[40] D. Furihata and T. Matsuo. *Discrete variational derivative method: a structure-preserving numerical method for partial differential equations*. CRC Press, 2010. doi: [10.1201/b10387](https://doi.org/10.1201/b10387).

[41] S. Gavrilyuk and K.-M. Shyue. "Hyperbolic approximation of the BBM equation." In: *Nonlinearity* 35.3 (2022), p. 1447. doi: [10.1088/1361-6544/ac4c49](https://doi.org/10.1088/1361-6544/ac4c49).

[42] J. Giesselmann and H. Ranocha. *Convergence of hyperbolic approximations to higher-order PDEs for smooth solutions*. Aug. 2025. arXiv: [2508.04112](https://arxiv.org/abs/2508.04112) [math.NA].

[43] T. J. Grant. "Bespoke finite difference schemes that preserve multiple conservation laws." In: *LMS Journal of Computation and Mathematics* 18.1 (2015), pp. 372–403. doi: [10.1112/S1461157015000078](https://doi.org/10.1112/S1461157015000078).

[44] E. Hairer. "Energy-preserving variant of collocation methods." In: *Journal of Numerical Analysis, Industrial and Applied Mathematics* 5 (2010), pp. 73–84.

[45] E. Hairer, C. Lubich, and G. Wanner. *Geometric Numerical Integration: Structure-Preserving Algorithms for Ordinary Differential Equations*. Vol. 31. Springer Series in Computational Mathematics. Berlin Heidelberg: Springer-Verlag, 2006. doi: [10.1007/3-540-30666-8](https://doi.org/10.1007/3-540-30666-8).

[46] P. Henning and D. Peterseim. "Crank-Nicolson Galerkin approximations to nonlinear Schrödinger equations with rough potentials." In: *Mathematical Models and Methods in Applied Sciences* 27.11 (2017), pp. 2147–2184. doi: [10.1142/S0218202517500415](https://doi.org/10.1142/S0218202517500415).

[47] J. Hietarinta. "Introduction to the Hirota bilinear method." In: *Integrability of Nonlinear Systems: Proceedings of the CIMPA School Pondicherry University, India, 8–26 January 1996*. Springer, 2007, pp. 95–103. doi: [10.1007/BFb0113694](https://doi.org/10.1007/BFb0113694).

[48] R. Hirota. "Exact solution of the Korteweg—de Vries equation for multiple collisions of solitons." In: *Physical Review Letters* 27.18 (1971), p. 1192. doi: [10.1103/PhysRevLett.27.1192](https://doi.org/10.1103/PhysRevLett.27.1192).

[49] S. G. Johnson. *Notes on FFT-based differentiation*. <https://math.mit.edu/~stevenj/fft-deriv.pdf>. 2011.

[50] W. B. Jones and J. J. O'Brien. "Pseudo-spectral methods and linear instabilities in reaction-diffusion fronts." In: *Chaos: An Interdisciplinary Journal of Nonlinear Science* 6.2 (1996), pp. 219–228. doi: [10.1063/1.166167](https://doi.org/10.1063/1.166167).

[51] S. Kang and E. M. Constantinescu. "Entropy-Preserving and Entropy-Stable Relaxation IMEX and Multirate Time-Stepping Methods." In: *Journal of Scientific Computing* 93 (2022), p. 23. doi: [10.1007/s10915-022-01982-w](https://doi.org/10.1007/s10915-022-01982-w). arXiv: [2108.08908](https://arxiv.org/abs/2108.08908) [math.NA].

[52] C. A. Kennedy and M. H. Carpenter. "Higher-order additive Runge-Kutta schemes for ordinary differential equations." In: *Applied Numerical Mathematics* 136 (2019), pp. 183–205. doi: [10.1016/j.apnum.2018.10.007](https://doi.org/10.1016/j.apnum.2018.10.007).

[53] D. I. Ketcheson. "Relaxation Runge-Kutta Methods: Conservation and Stability for Inner-Product Norms." In: *SIAM Journal on Numerical Analysis* 57.6 (2019), pp. 2850–2870. doi: [10.1137/19M1263662](https://doi.org/10.1137/19M1263662). arXiv: [1905.09847](https://arxiv.org/abs/1905.09847) [math.NA].

[54] J. Klement. "On Using Quasi-Newton Algorithms of the Broyden Class for Model-to-test Correlation." In: *Journal of Aerospace Technology and Management* 6.4 (2014), pp. 407–414. doi: [10.5028/jatm.v6i4.373](https://doi.org/10.5028/jatm.v6i4.373).

[55] S. Koide and D. Furihata. "Nonlinear and linear conservative finite difference schemes for regularized long wave equation." In: *Japan Journal of Industrial and Applied Mathematics* 26.1 (2009), p. 15. doi: [10.1007/BF03167544](https://doi.org/10.1007/BF03167544).

[56] D. A. Kopriva. *Implementing Spectral Methods for Partial Differential Equations: Algorithms for Scientists and Engineers*. New York: Springer Science & Business Media, 2009. doi: [10.1007/978-90-481-2261-5](https://doi.org/10.1007/978-90-481-2261-5).

[57] D. J. Korteweg and G. De Vries. "On the change of form of long waves advancing in a rectangular canal, and on a new type of long stationary waves." In: *The London, Edinburgh, and Dublin Philosophical Magazine and Journal of Science* 39.240 (1895), pp. 422–443. doi: [10.1080/14786449508620739](https://doi.org/10.1080/14786449508620739).

[58] J. Lampert and H. Ranocha. "Structure-Preserving Numerical Methods for Two Nonlinear Systems of Dispersive Wave Equations." In: *Computational Science and Engineering* 2 (Nov. 2025), p. 2. doi: [10.1007/s44207-025-00006-3](https://doi.org/10.1007/s44207-025-00006-3). arXiv: [2402.16669](https://arxiv.org/abs/2402.16669) [math.NA].

[59] D. Li and X. Li. "Relaxation Exponential Rosenbrock-Type Methods for Oscillatory Hamiltonian Systems." In: *SIAM Journal on Scientific Computing* 45.6 (2023), A2886–A2911. doi: [10.1137/22M1511345](https://doi.org/10.1137/22M1511345).

[60] D. Li, X. Li, and Z. Zhang. "Implicit-explicit relaxation Runge-Kutta methods: construction, analysis and applications to PDEs." In: *Mathematics of Computation* (2022). doi: [10.1090/mcom/3766](https://doi.org/10.1090/mcom/3766).

[61] H. Li, X. Li, K. Schratz, and B. Wang. *Time-Relaxation Structure-Preserving Explicit Low-Regularity Integrators for the Nonlinear Schrödinger Equation*. 2025. arXiv: [2510.02963](https://arxiv.org/abs/2510.02963) [math.NA].

[62] X. Li, Y. Gong, and L. Zhang. "Linear high-order energy-preserving schemes for the nonlinear Schrödinger equation with wave operator using the scalar auxiliary variable approach." In: *Journal of Scientific Computing* 88.1 (2021), p. 20. doi: [10.1007/s10915-021-01533-9](https://doi.org/10.1007/s10915-021-01533-9).

[63] V. Linders, H. Ranocha, and P. Birken. "Resolving Entropy Growth from Iterative Methods." In: *BIT Numerical Mathematics* 63 (4 Sept. 2023). doi: [10.1007/s10543-023-00992-w](https://doi.org/10.1007/s10543-023-00992-w). arXiv: [2302.13579](https://arxiv.org/abs/2302.13579) [math.NA].

[64] Y. Maday and A. Quarteroni. "Error analysis for spectral approximation of the Korteweg-de Vries equation." In: *ESAIM: Mathematical Modelling and Numerical Analysis* 22.3 (1988), pp. 499–529. doi: [10.1051/m2an/1988220304991](https://doi.org/10.1051/m2an/1988220304991).

[65] R. I. McLachlan, G. Quispel, and N. Robidoux. "Geometric integration using discrete gradients." In: *Philosophical Transactions of the Royal Society of London. Series A: Mathematical, Physical and Engineering Sciences* 357.1754 (1999), pp. 1021–1045. doi: [10.1098/rsta.1999.0363](https://doi.org/10.1098/rsta.1999.0363).

[66] D. Mitsotakis, H. Ranocha, D. I. Ketcheson, and E. Süli. "A conservative fully-discrete numerical method for the regularized shallow water wave equations." In: *SIAM Journal on Scientific Computing* 42 (2 Apr. 2021), B508–B537. doi: [10.1137/20M1364606](https://doi.org/10.1137/20M1364606). arXiv: [2009.09641](https://arxiv.org/abs/2009.09641) [math.NA].

[67] R. M. Miura, C. S. Gardner, and M. D. Kruskal. "Korteweg-de Vries equation and generalizations. II. Existence of conservation laws and constants of motion." In: *Journal of Mathematical Physics* 9.8 (1968), pp. 1204–1209. doi: [10.1063/1.1664701](https://doi.org/10.1063/1.1664701).

[68] W. Moses and V. Churavy. "Instead of rewriting foreign code for machine learning, automatically synthesize fast gradients." In: *Advances in Neural Information Processing Systems* 33 (2020), pp. 12472–12485.

[69] W. S. Moses, V. Churavy, L. Paehler, J. Hückelheim, S. H. K. Narayanan, M. Schanen, and J. Doerfert. "Reverse-mode automatic differentiation and optimization of GPU kernels via Enzyme." In: *Proceedings of the International Conference for High Performance Computing, Networking, Storage and Analysis*. 2021, pp. 1–16. doi: [10.1145/3458817.3476165](https://doi.org/10.1145/3458817.3476165).

[70] P. J. Olver. "Euler operators and conservation laws of the BBM equation." In: *Mathematical Proceedings of the Cambridge Philosophical Society*. Vol. 85. 1. Cambridge University Press. 1979, pp. 143–160. doi: [10.1017/S0305004100055572](https://doi.org/10.1017/S0305004100055572).

[71] S. A. Orszag. "On the elimination of aliasing in finite-difference schemes by filtering high-wavenumber components." In: *Journal of Atmospheric Sciences* 28.6 (1971), pp. 1074–1074. doi: [10.1175/1520-0469\(1971\)028<1074:OTE0AI>2.0.CO;2](https://doi.org/10.1175/1520-0469(1971)028<1074:OTE0AI>2.0.CO;2).

[72] A. Pal, F. Holtorf, A. Larsson, T. Loman, Utkarsh, F. Schäfer, Q. Qu, A. Edelman, and C. Rackauckas. "NonlinearSolve.jl: High-Performance and Robust Solvers for Systems of Nonlinear Equations in Julia." In: (2024). doi: [10.48550/arXiv.2403.16341](https://doi.org/10.48550/arXiv.2403.16341). arXiv: [2403.16341](https://arxiv.org/abs/2403.16341) [math.NA].

[73] G. Quispel and D. I. McLaren. "A new class of energy-preserving numerical integration methods." In: *Journal of Physics A: Mathematical and Theoretical* 41.4 (2008), p. 045206. doi: [10.1088/1751-8113/41/4/045206](https://doi.org/10.1088/1751-8113/41/4/045206).

[74] H. Ranocha. "SummationByPartsOperators.jl: A Julia library of provably stable semidiscretization techniques with mimetic properties." In: *Journal of Open Source Software* 6.64 (Aug. 2021), p. 3454. doi: [10.21105/joss.03454](https://doi.org/10.21105/joss.03454). URL: <https://github.com/ranocha/SummationByPartsOperators.jl>.

[75] H. Ranocha, L. Dalcin, and M. Parsani. "Fully-Discrete Explicit Locally Entropy-Stable Schemes for the Compressible Euler and Navier-Stokes Equations." In: *Computers and Mathematics with Applications* 80.5 (July 2020), pp. 1343–1359. doi: [10.1016/j.camwa.2020.06.016](https://doi.org/10.1016/j.camwa.2020.06.016). arXiv: [2003.08831](https://arxiv.org/abs/2003.08831) [math.NA].

[76] H. Ranocha and D. I. Ketcheson. "Energy Stability of Explicit Runge-Kutta Methods for Nonautonomous or Nonlinear Problems." In: *SIAM Journal on Numerical Analysis* 58.6 (Nov. 2020), pp. 3382–3405. doi: [10.1137/19M1290346](https://doi.org/10.1137/19M1290346). arXiv: [1909.13215](https://arxiv.org/abs/1909.13215) [math.NA].

[77] H. Ranocha and D. I. Ketcheson. *High-order mass- and energy-conserving methods for the nonlinear Schrödinger equation and its hyperbolization*. Oct. 2025. arXiv: [2510.14335](https://arxiv.org/abs/2510.14335) [math.NA].

[78] H. Ranocha and D. I. Ketcheson. "Relaxation Runge-Kutta Methods for Hamiltonian Problems." In: *Journal of Scientific Computing* 84.1 (July 2020). doi: [10.1007/s10915-020-01277-y](https://doi.org/10.1007/s10915-020-01277-y). arXiv: [2001.04826](https://arxiv.org/abs/2001.04826) [math.NA].

[79] H. Ranocha and D. I. Ketcheson. *Reproducibility repository for "Conserving mass, momentum, and energy for the Benjamin-Bona-Mahony, Korteweg-de Vries, and nonlinear Schrödinger equations"*. https://github.com/ranocha/2025_BBM_KdV_NLS. 2025. doi: [10.5281/zenodo.17936837](https://doi.org/10.5281/zenodo.17936837).

[80] H. Ranocha, L. Lóczi, and D. I. Ketcheson. "General Relaxation Methods for Initial-Value Problems with Application to Multistep Schemes." In: *Numerische Mathematik* 146 (Oct. 2020), pp. 875–906. doi: [10.1007/s00211-020-01158-4](https://doi.org/10.1007/s00211-020-01158-4). arXiv: [2003.03012](https://arxiv.org/abs/2003.03012) [math.NA].

[81] H. Ranocha, D. Mitsotakis, and D. I. Ketcheson. "A Broad Class of Conservative Numerical Methods for Dispersive Wave Equations." In: *Communications in Computational Physics* 29.4 (Feb. 2021), pp. 979–1029. doi: [10.4208/cicp.0A-2020-0119](https://doi.org/10.4208/cicp.0A-2020-0119). arXiv: [2006.14802](https://arxiv.org/abs/2006.14802) [math.NA].

[82] H. Ranocha and M. Ricchiuto. "Structure-preserving approximations of the Serre-Green-Naghdi equations in standard and hyperbolic form." In: *Numerical Methods for Partial Differential Equations* 41.4 (June 2025), e70016. doi: [10.1002/num.70016](https://doi.org/10.1002/num.70016). arXiv: [2408.02665](https://arxiv.org/abs/2408.02665) [math.NA].

[83] H. Ranocha, M. Sayyari, L. Dalcin, M. Parsani, and D. I. Ketcheson. "Relaxation Runge-Kutta Methods: Fully-Discrete Explicit Entropy-Stable Schemes for the Compressible Euler and Navier-Stokes Equations." In: *SIAM Journal on Scientific Computing* 42.2 (Mar. 2020), A612–A638. doi: [10.1137/19M1263480](https://doi.org/10.1137/19M1263480). arXiv: [1905.09129](https://arxiv.org/abs/1905.09129) [math.NA].

[84] H. Ranocha and J. Schütz. "Multiderivative time integration methods preserving nonlinear functionals via relaxation." In: *Communications in Applied Mathematics and Computational Science* 19 (1 June 2024), pp. 27–56. doi: [10.2140/camcos.2024.19.27](https://doi.org/10.2140/camcos.2024.19.27). arXiv: 2311.03883 [math.NA].

[85] H. Ranocha, J. Schütz, and E. Theodosiou. "Functional-preserving predictor-corrector multiderivative schemes." In: *Proceedings in Applied Mathematics and Mechanics* (Sept. 2023). doi: [10.1002/pamm.202300025](https://doi.org/10.1002/pamm.202300025). arXiv: 2308.04876 [math.NA].

[86] J. M. Sanz-Serna. "An explicit finite-difference scheme with exact conservation properties." In: *Journal of Computational Physics* 47.2 (1982), pp. 199–210. doi: [10.1016/0021-9991\(82\)90074-2](https://doi.org/10.1016/0021-9991(82)90074-2).

[87] J. M. Sanz-Serna. "Methods for the numerical solution of the nonlinear Schrödinger equation." In: *Mathematics of Computation* 43.167 (1984), pp. 21–27. doi: [10.1090/S0025-5718-1984-0744922-X](https://doi.org/10.1090/S0025-5718-1984-0744922-X).

[88] E. Schulz and A. T. Wan. "Minimal ℓ^2 norm discrete multiplier method." In: *Journal of Computational Dynamics* 12.2 (2025), pp. 212–238. doi: [10.3934/jcd.2024029](https://doi.org/10.3934/jcd.2024029).

[89] C. Sulem and P.-L. Sulem. *The nonlinear Schrödinger equation: self-focusing and wave collapse*. Vol. 139. Springer Science & Business Media, 2007. doi: [10.1007/b98958](https://doi.org/10.1007/b98958).

[90] M. Svärd and J. Nordström. "Review of summation-by-parts schemes for initial-boundary-value problems." In: *Journal of Computational Physics* 268 (2014), pp. 17–38. doi: [10.1016/j.jcp.2014.02.031](https://doi.org/10.1016/j.jcp.2014.02.031).

[91] E. Tadmor. "Entropy stability theory for difference approximations of nonlinear conservation laws and related time-dependent problems." In: *Acta Numerica* 12 (2003), pp. 451–512. doi: [10.1017/S0962492902000156](https://doi.org/10.1017/S0962492902000156).

[92] E. Tadmor. "The numerical viscosity of entropy stable schemes for systems of conservation laws. I." In: *Mathematics of Computation* 49.179 (1987), pp. 91–103. doi: [10.1090/S0025-5718-1987-0890255-3](https://doi.org/10.1090/S0025-5718-1987-0890255-3).

[93] A. T. Wan, A. Bihlo, and J.-C. Nave. "The multiplier method to construct conservative finite difference schemes for ordinary and partial differential equations." In: *SIAM Journal on Numerical Analysis* 54.1 (2016), pp. 86–119. doi: [10.1137/140997944](https://doi.org/10.1137/140997944).

[94] G. Yan, S. Kaur, J. E. Hicken, and J. W. Banks. "Entropy-stable Galerkin difference discretization on unstructured grids." In: *AIAA AVIATION 2020 FORUM*. 2020, p. 3033. doi: [10.2514/6.2020-3033](https://doi.org/10.2514/6.2020-3033).

[95] J. Yang. *Nonlinear waves in integrable and nonintegrable systems*. SIAM, 2010. doi: [10.1137/1.9780898719680](https://doi.org/10.1137/1.9780898719680).

[96] K. Yang. "Arbitrarily High-Order Conservative Schemes for the Generalized Korteweg-de Vries Equation." In: *SIAM Journal on Scientific Computing* 44.4 (2022), A2709–A2733. doi: [10.1137/21M140777X](https://doi.org/10.1137/21M140777X).

[97] H. Zhang, X. Qian, J. Yan, and S. Song. "Highly efficient invariant-conserving explicit Runge-Kutta schemes for nonlinear Hamiltonian differential equations." In: *Journal of Computational Physics* (2020), p. 109598. doi: [10.1016/j.jcp.2020.109598](https://doi.org/10.1016/j.jcp.2020.109598).

[98] W. Zheng and Y. Xu. "Invariants Preserving Time-Implicit Local Discontinuous Galerkin Schemes for High-Order Nonlinear Wave Equations." In: *Communications on Applied Mathematics and Computation* (2024), pp. 1–28. doi: [10.1007/s42967-024-00420-y](https://doi.org/10.1007/s42967-024-00420-y).